

# **The Effects of Organophosphate Esters used as Flame Retardants and Plasticizers on Granulosa, Leydig, and Spermatogonial Cells Analyzed Using High-Content Imaging**

Xiaotong Wang, Trang Luu, Marc A. Beal, Tara S. Barton-Maclaren, Bernard Robaire, Barbara F. Hales

## **Supplementary Files**

1. Supplementary Methods

2. Supplementary Data

Table S1. Supplementary Table S1. Cell permeable fluorescent dye combinations used in high-content imaging experiments.

Table S2. Parameters used in High-Throughput Toxicokinetics (HTTK) modelling and the steady-state concentration ( $C_{ss}$ ) values of chemicals of interest.

Table S3. Benchmark concentrations (BMCs) of flame retardant chemicals for each endpoint in KGN, MA-10, and C18-4 cells.

Table S4. Administered Equivalent Doses (AEDs) of flame retardant chemicals for each endpoint in KGN, MA-10, and C18-4 cells.

Figure S1. Effects of BDE-47 and OPEs on the intensity of mitochondrial staining.

Figure S2. Effects of BDE-47 and OPEs on the ratio of active to total mitochondria.

Figure S3. Effects of BDE-47 and OPEs on the intensity of LysoTracker Red staining.

Figure S4-S14. Quantification data, with a full concentration range of all parameters for each individual chemical.

Figure S15. Correlation matrices showing relationships between phenotypic endpoints for each individual chemical.

Figure S16. Clustering dendrograms based on chemical-specific ToxPi profiles.

## Supplementary Methods

### Columbus Image Analyses – KGN cells

Input image – individual plane, or maximum projection if multiple focal planes were screened (i.e., Z-stack); flatfield correction – advanced, or basic if advanced mode is not applicable.

#### *Combination 1 – Hoechst/Calcein-AM/Lysotracker Red*

The nuclei were identified by Hoechst staining using the function [Find Nuclei] – (channel: Hoechst 33342; method B, common threshold = 0.2, area > 30  $\mu\text{m}^2$ , split factor = 7, individual threshold = 0.5, contrast > 0.1). The nuclear morphology was assessed: [Calculate Morphology Properties] – (population: nuclei, region: nucleus; method standard: area ( $\mu\text{m}^2$ ) and roundness); [Calculate Intensity Properties] – (channel: Hoechst 33342, population: nuclei, region: nucleus; method standard, mean). A sub-population of nuclei was selected to exclude potential non-nuclear staining and extreme outliers: [Select Population] – (population: nuclei; method filter by properties: filter F1 = intensity < 5,000-6,000 (the median nucleus intensity was ~2,000-3,000), filter F2 = nuclear area < 500  $\mu\text{m}^2$ ). The cytoplasmic areas were identified by Calcein staining: [Find Cytoplasm] – (channel: Calcein green, nuclei selected; method A, individual threshold = 0.05). The lysosomes were defined: [Find Spots] – (channel: Lysotracker Red, region of interest (ROI) population: nuclei selected, ROI region: cell; method A, relative spot intensity > 0.075, splitting coefficient = 1). The morphological features of lysosomes and the mean staining intensity were assessed: [Calculate Morphology Properties (2)] – (population: nuclei selected, region: cell; method standard: area ( $\mu\text{m}^2$ ) and roundness); [Calculate Intensity Properties (2)] – (channel: Lysotracker Red, population: spots, region: spot maximum; method standard, mean). The intensity of Calcein staining was assessed: [Calculate Intensity Properties (3)] – (channel: Calcein green, population: nuclei selected, region: cytoplasm; method standard, mean). The Calcein-positive viable cells were defined by [Select Population (2)] – (population: nuclei selected; method filter by properties: filter F1 = intensity > 500). A sub-population of lysosomes was selected to exclude potential non-lysosomal staining and extreme outliers: [Select Population] – (population: spots; method filter by properties: filter F1 = intensity < 8,000-12,000, filter F2 = spot area < 200  $\text{px}^2$ ). The outputs of combination 1 included: the number of nuclei,

the Calcein-positive ratio (i.e., the number of Calcein-positive cells divided by the total number of selected nuclei), Calcein intensity, the number of lysosomes per cell (calculated by dividing the total numbers of selected spots by the total number of selected nuclei), the average intensity of Lysotracker Red staining.

#### *Combination 2 – Hoechst/Mitotracker Green/Mitotracker Red/Cellmask*

The nuclei were identified by Hoechst staining: [Find Nuclei] – (channel: Hoechst 33342; method B, common threshold = 0.2, area > 30  $\mu\text{m}^2$ , split factor = 17, individual threshold = 0.2, contrast > 0.1). The nuclear morphology was assessed: [Calculate Morphology Properties] – (population: nuclei, region: nucleus; method standard: area ( $\mu\text{m}^2$ ) and roundness); [Calculate Intensity Properties] – (channel: Hoechst 33342, population: nuclei, region: nucleus; method standard, mean). A sub-population of nuclei was selected to exclude potential non-nuclear staining and extreme outliers: [Select Population] – (population: nuclei; method filter by properties: filter F1 = intensity < 5,000-6,000, filter F2 = nuclear area < 500  $\mu\text{m}^2$ ). The cytoplasmic areas were identified by Cellmask staining: [Find Cytoplasm] – (channel: Cellmask Deep Red, nuclei selected; method F, individual threshold = 0.15). The regions of mitochondria were defined: [Find Image Region] – (channel: Mitotracker Green, ROI population: nuclei selected, ROI region: cell; method common threshold = 0.35, split into objects, area > 0  $\text{px}^2$ ). The mean staining intensity of mitochondria was assessed: [Calculate Intensity Properties (2)] – (channel: Mitotracker Green, population: mitogreen, region: mitochondria; method standard, mean); [Calculate Intensity Properties (3)] – (channel: Mitotracker Red, population: mitored, region: mitochondria; method standard, mean). The outputs of combination 2 included: the number of nuclei, the average intensity of Mitotracker Green staining, the average intensity of Mitotracker Red staining, the active to total mitochondria ratio (calculated by the average intensity of Mitotracker Red/Mitotracker Green).

#### *Combination 3 – Hoechst/Calcein-AM/CellROX*

The nuclei were identified by Hoechst staining: [Find Nuclei] – (channel: Hoechst 33342; method B, common threshold = 0.4, area > 30  $\mu\text{m}^2$ , split factor = 7, individual threshold = 0.4, contrast > 0.1). The nuclear morphology was assessed: [Calculate Morphology Properties] – (population: nuclei, region: nucleus; method standard: area ( $\mu\text{m}^2$ ) and

roundness); [Calculate Intensity Properties] – (channel: Hoechst 33342, population: nuclei, region: nucleus; method standard, mean). A sub-population of nuclei was selected to exclude potential non-nuclear staining and extreme outliers: [Select Population] – (population: nuclei; method filter by properties: filter F1 = intensity < 5,000-6,000, filter F2 = nuclear area < 500  $\mu\text{m}^2$ ). The cytoplasmic areas were identified by Calcein staining: [Find Cytoplasm] – (channel: Calcein green, nuclei selected; method A, individual threshold = 0.05). The cell surrounding region was determined and marked as background: [Find Surrounding Region] – (channel: Calcein green, population: nuclei selected, region: cell; method A, individual threshold = 0.15). The intensity of CellROX in the cytoplasmic and the background regions was assessed: [Calculate Intensity Properties] – (channel: CellROX, population: nuclei selected, region: cell or background; method standard, mean). The corrected CellROX intensity was calculated by subtracting Intensity Background CellROX from Intensity Cell CellROX. The outputs of combination 3 included: the number of nuclei, the corrected intensity of CellROX staining.

#### *Combination 4 – Hoechst/Nile Red/Cellmask*

The nuclei were identified by Hoechst staining: [Find Nuclei] – (channel: Hoechst 33342; method B, common threshold = 0.4, area > 30  $\mu\text{m}^2$ , split factor = 7, individual threshold = 0.4, contrast > 0.1). The nuclear morphology was assessed: [Calculate Morphology Properties] – (population: nuclei, region: nucleus; method standard: area ( $\mu\text{m}^2$ ) and roundness); [Calculate Intensity Properties] – (channel: Hoechst 33342, population: nuclei, region: nucleus; method standard, mean). A sub-population of nuclei was selected to exclude potential non-nuclear staining and extreme outliers: [Select Population] – (population: nuclei; method filter by properties: filter F1 = intensity < 5,000-6,000, filter F2 = nuclear area < 500  $\mu\text{m}^2$ ). The cytoplasmic areas were identified by Cellmask staining: [Find Cytoplasm] – (channel: Cellmask Deep Red, nuclei selected; method A, individual threshold = 0.05). The lipid droplets were localized: [Find Spots] – (channel: Nile Red, ROI population: nuclei selected, ROI region: cell; method A, relative spot intensity > 0.080, splitting coefficient = 1). The outputs of combination 4 included: the number of nuclei, the total area and the average number of lipid droplets per cell.

## Supplementary Data

Supplementary Table S1. Cell permeable fluorescent dye combinations used in high-content imaging experiments.

Dye	Staining	Dilution	Comb1	Comb2	Comb3	Comb4
Hoechst 33342	Nuclei	1:2000	✓	✓	✓	✓
Calcein-AM	Cell viability, cytoplasm	1:1000	✓		✓	
CellROX Deep Red	Reactive oxygen species (oxidative stress)	1:2500			✓	
MitoTracker Green FM	Total mitochondria	1:2000		✓		
MitoTracker Red CM-H2XRos	Active mitochondria	1:2500		✓		
LysoTracker Red DND-99	Lysosomes	1:6000	✓			
Nile Red	Lipid droplets	1:100				✓
CellMask Deep Red	Plasma membrane	1:1000		✓		✓

Combination (comb) 1, 2, and 3 were prepared with incomplete medium (phenol-red free DMEM/F-12 or DMEM), while combination 4 was prepared with 2% (w/v) polyvinylpyrrolidone. For combination 1, 3, and 4, half (100  $\mu$ l) of the exposure medium was removed from each well, 50  $\mu$ l of the corresponding dye solution was added. For combination 2, all of the medium was removed and 150  $\mu$ l of the dye solution was added to minimize the interaction between serum and MitoTracker Green. The final dilution factors for each dye in the combinations are indicated in the Table. The cells were stained for 30 minutes, and then washed once with 200  $\mu$ l of incomplete medium; 100  $\mu$ l of incomplete medium was added to each well for live-cell imaging. w/v: weight/volume percent.

Supplementary Table S2. Parameters used in High-Throughput Toxicokinetics (HTTK) modelling and the steady-state concentration ( $C_{ss}$ ) values of chemicals of interest.

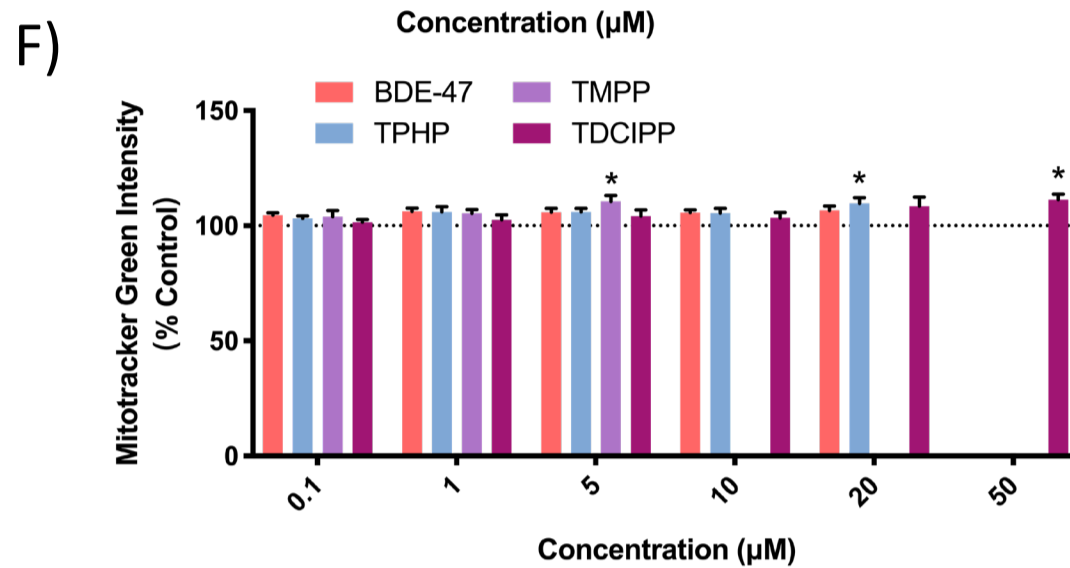
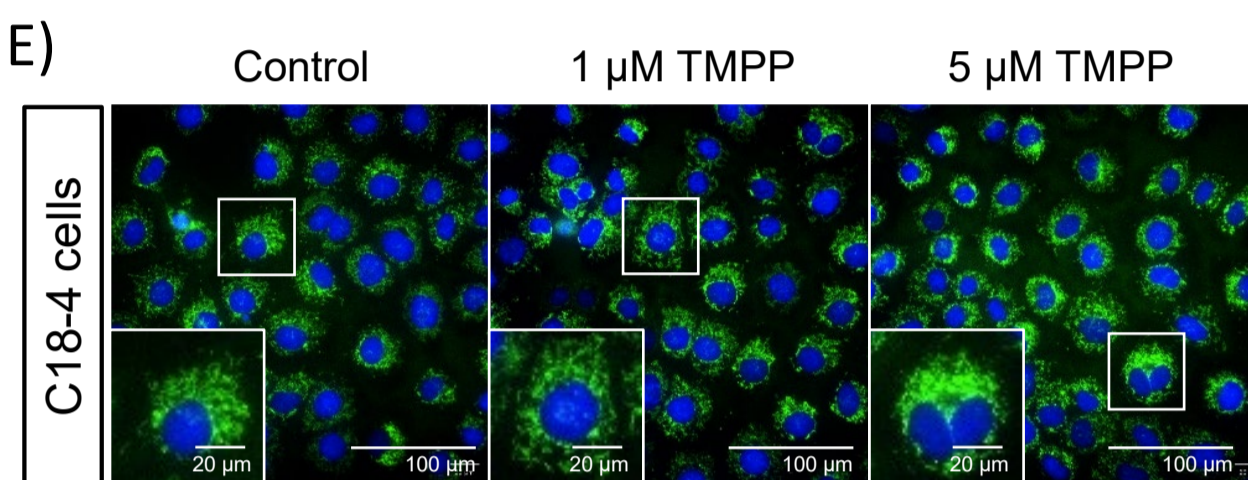
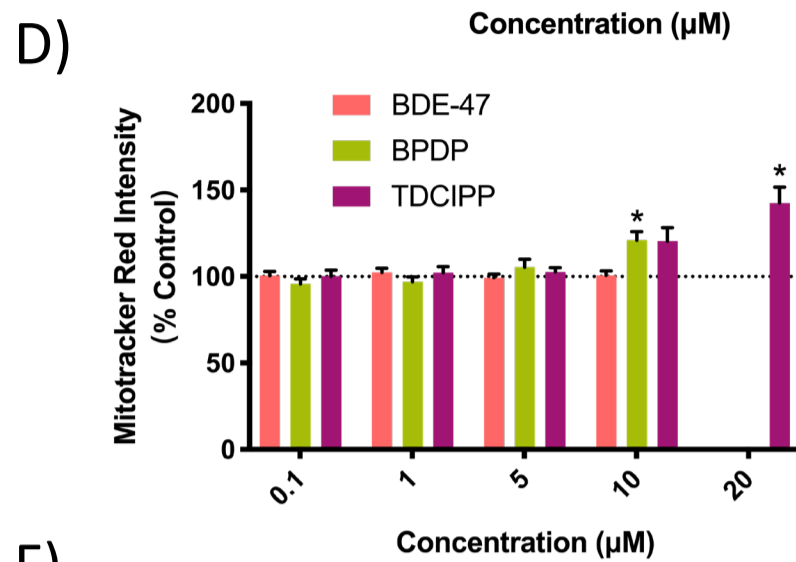
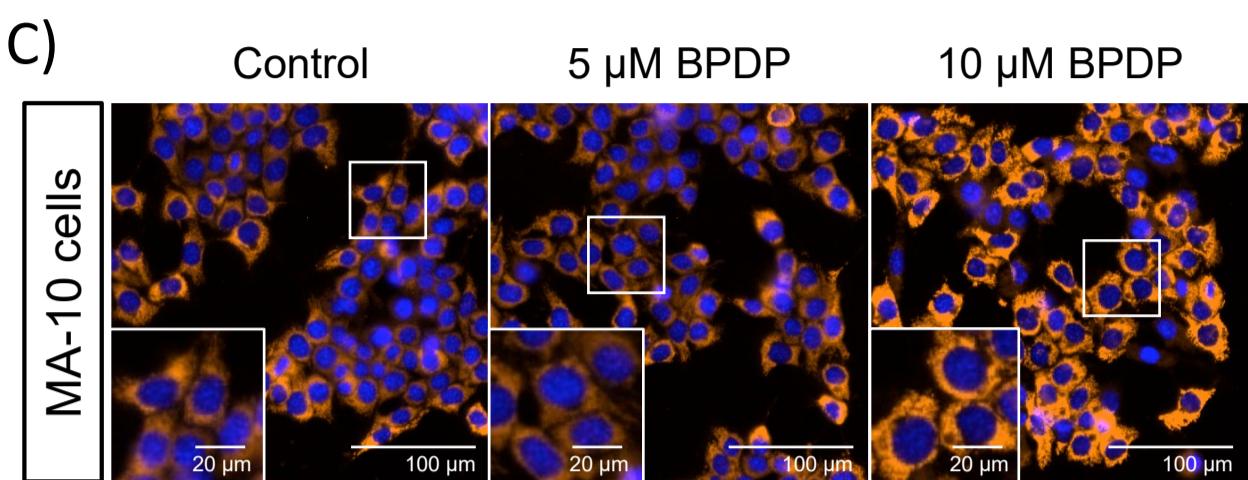
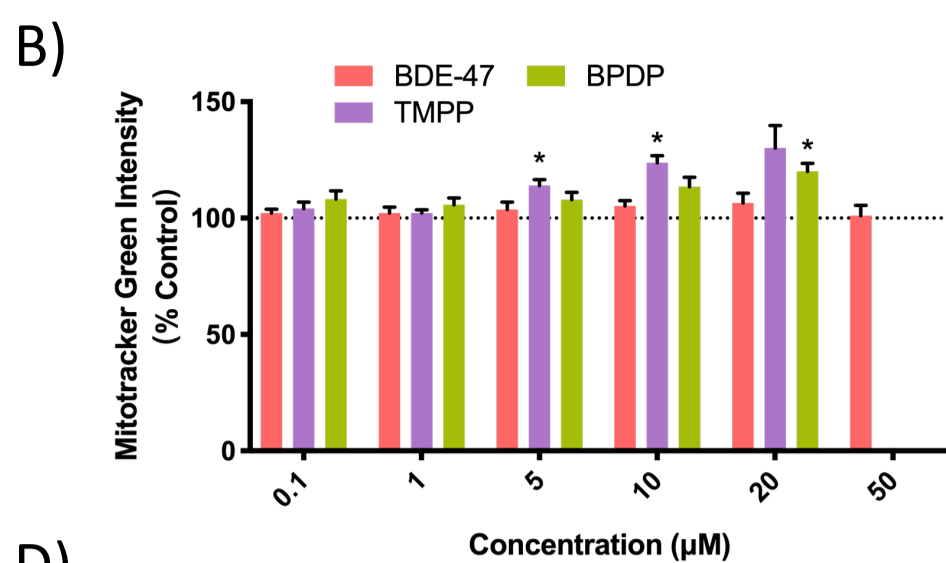
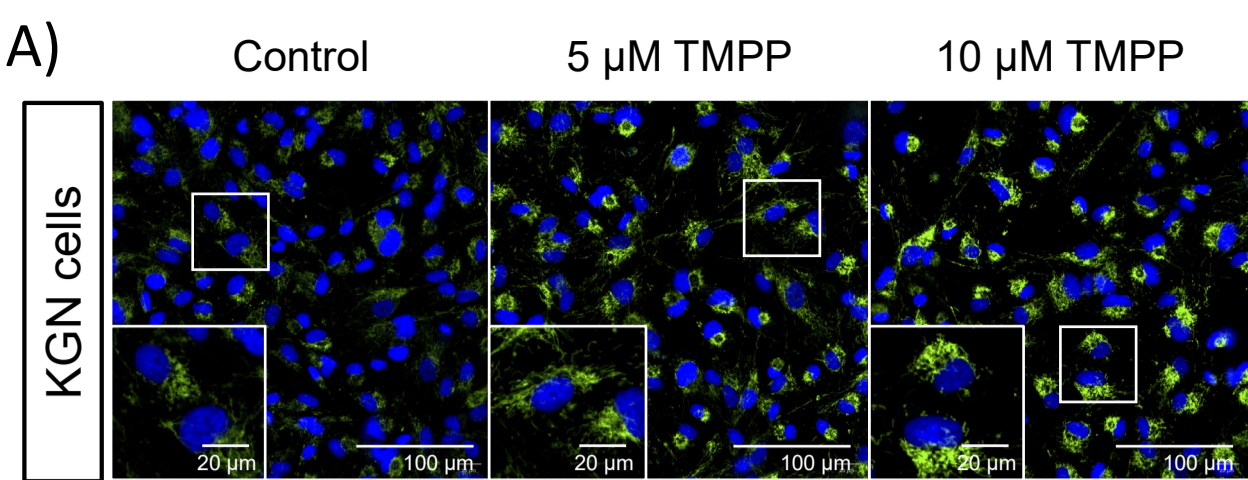
<b>Acronym</b>	<b>Cas#</b>	<b>LogP</b>	<b>M.W.</b>	<b>Human.Clint</b>	<b>Human.Funbound.plasma</b>	<b><math>C_{ss}</math></b>
BDE-47	5436-43-1	6.81	485.795	2.230921	0.0187	55.8
TPHP <sup>1</sup>	115-86-6	4.589	326.3	26.44	0.002852	89.67
TMPP	1330-78-5	5.11	368.4	2.99254	0.0004	1008
IPPP <sup>1,3</sup>	68937-41-7	9.4	452.5	138.4571	0.023353	N/A
BPDP <sup>1</sup>	56803-37-3	5.12	382.4	35.31819	0.034492	43.21
TDtBPP <sub>1,2,3</sub>	95906-11-9	10.5	662.936	2841.561	0.067907	N/A
BDMPP <sub>1,2,3</sub>	69284-93-1	7.58	474.622	99.63774	0.053714	N/A
TBOEP <sup>1</sup>	78-51-3	3.749	398.5	6.860755	0.24436	47.66
TDCIPP <sup>1</sup>	13674-87-8	3.65	430.9	5.092	0.01078	136.3
TCIPP	13674-84-5	2.592	327.6	1.925409	0.1434	23.15

Parameters used in High-Throughput Toxicokinetics (HTTK) modelling and the steady-state concentration ( $C_{ss}$ ) values of chemicals of interest. N/A: non-available/applicable; LogKow: octanol/water partition coefficients; M.W.: molecular weight; Clint: intrinsic clearance; Funbound.plasma: fraction unbound in the plasma protein.

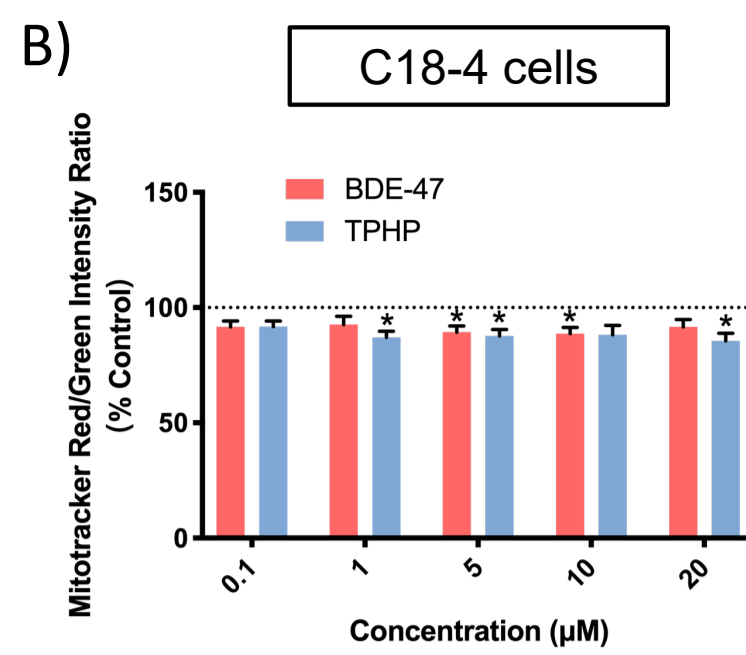
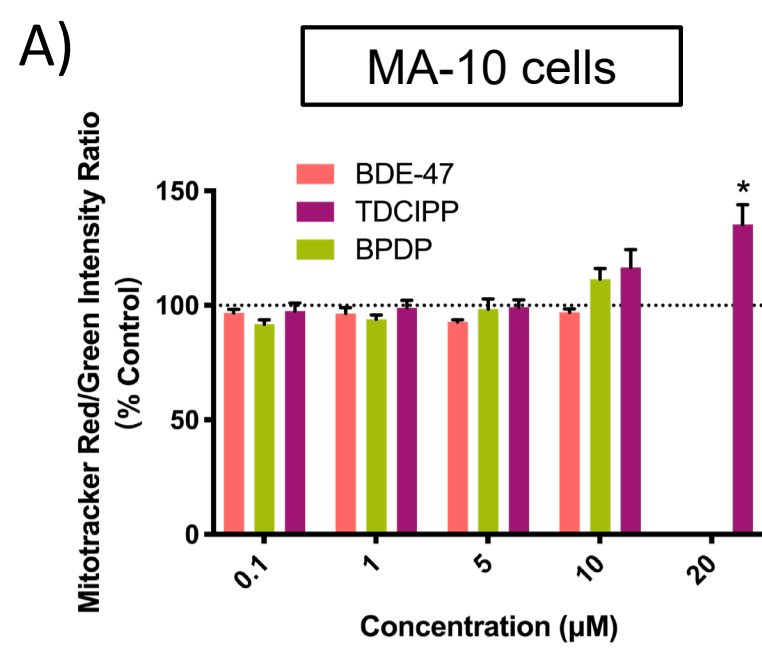
<sup>1</sup> Compounds that are already in the HTTK database; no additional data input for IVIVE modelling was required.

<sup>2</sup> Compounds that are outside the domain of applicability of ADMET prediction algorithms.

<sup>3</sup> Compounds that have high LogKow and clearance values.

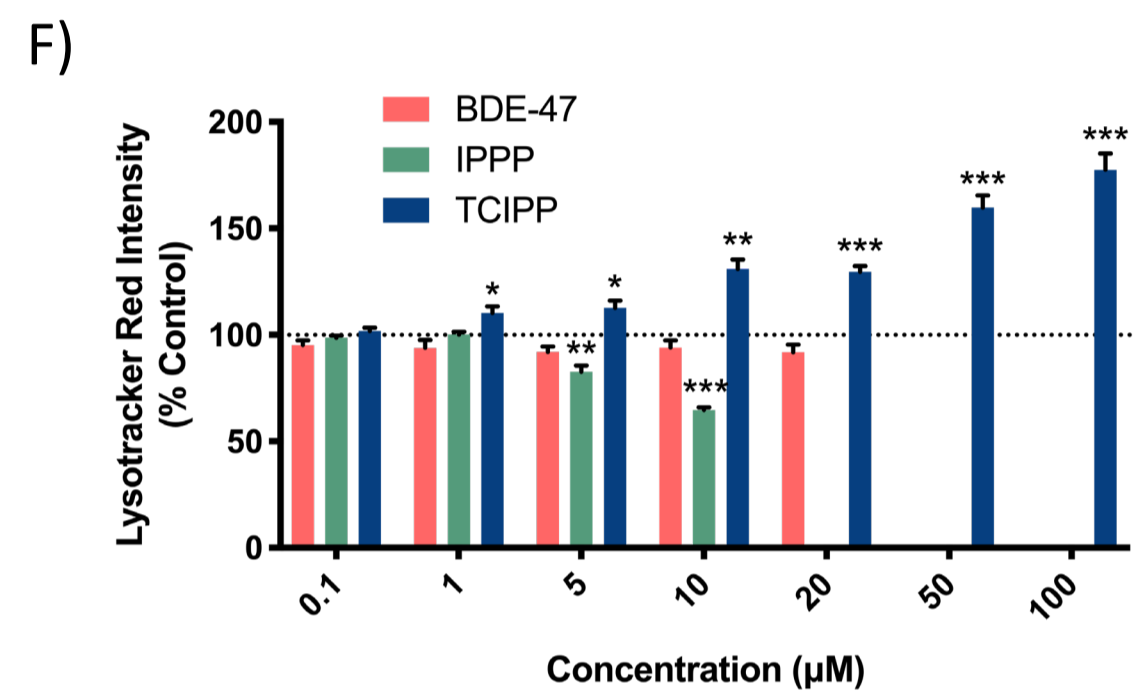
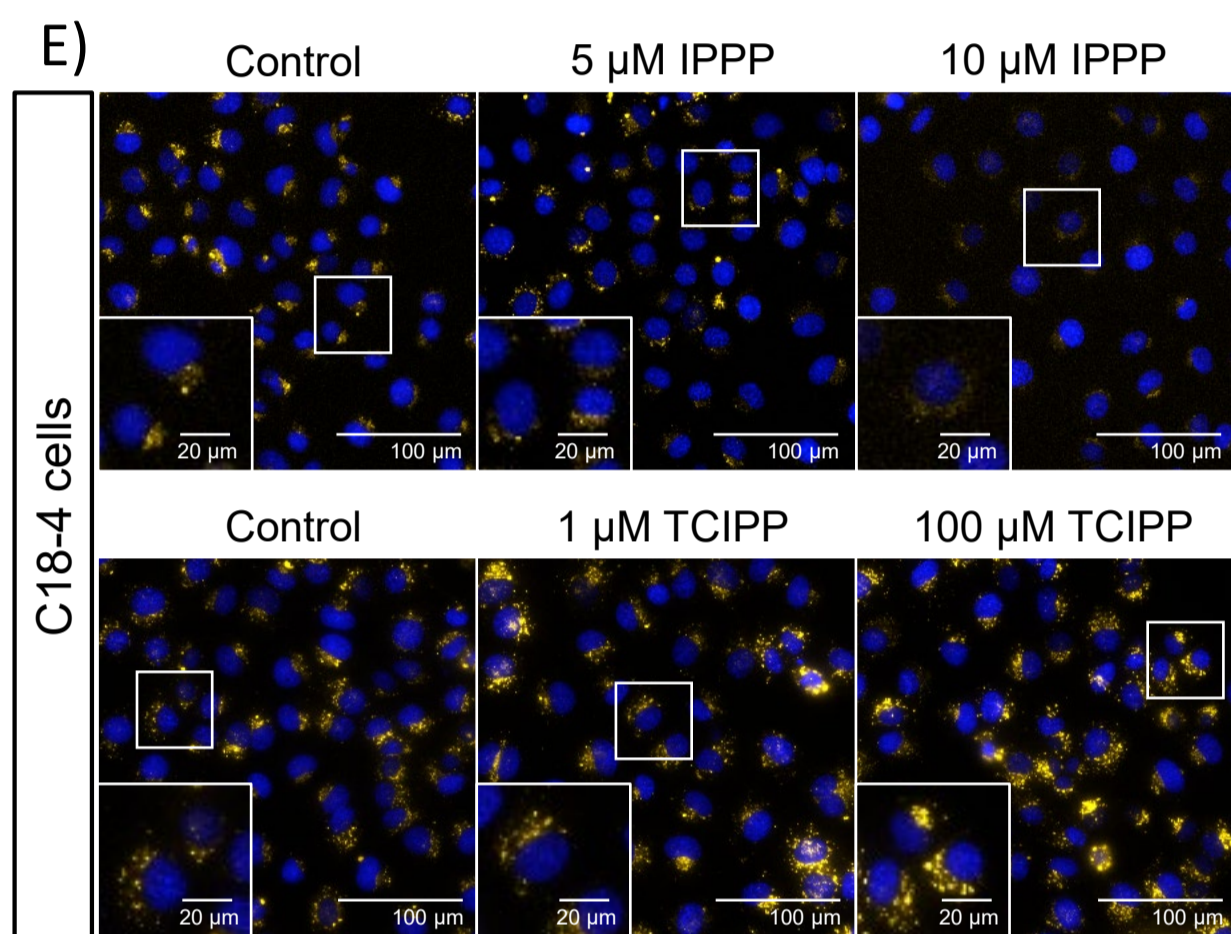
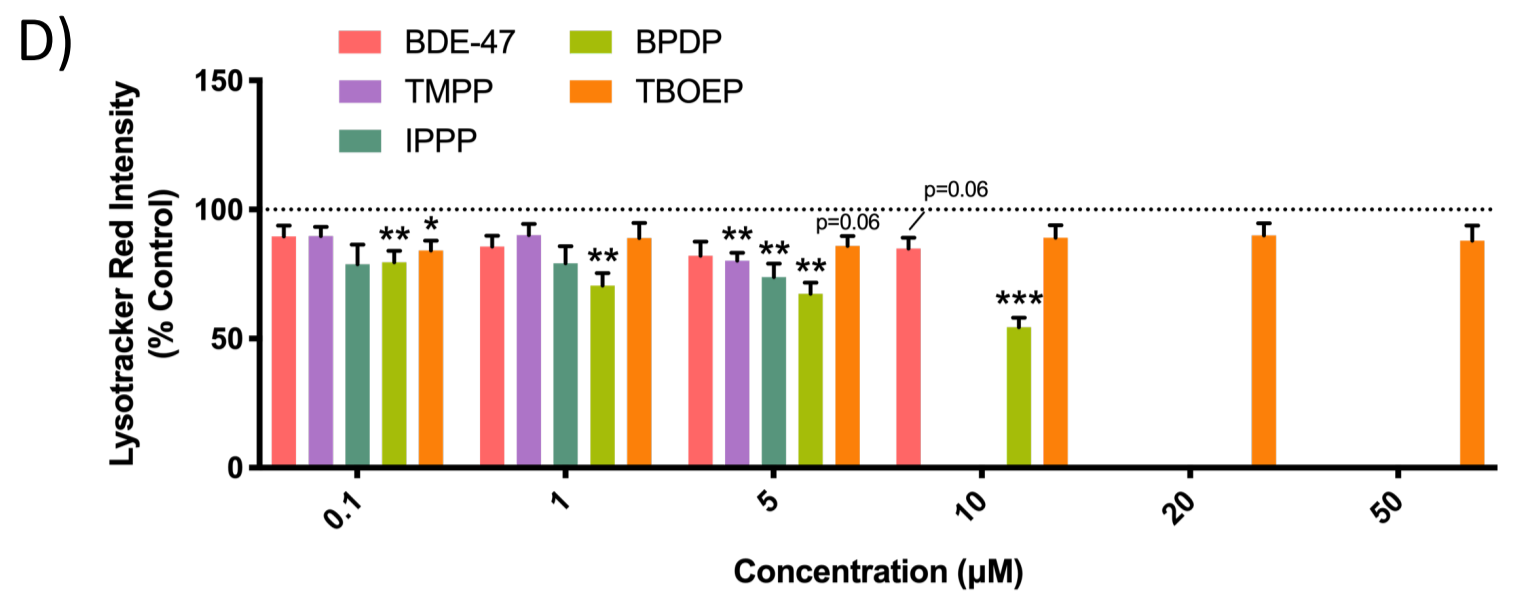
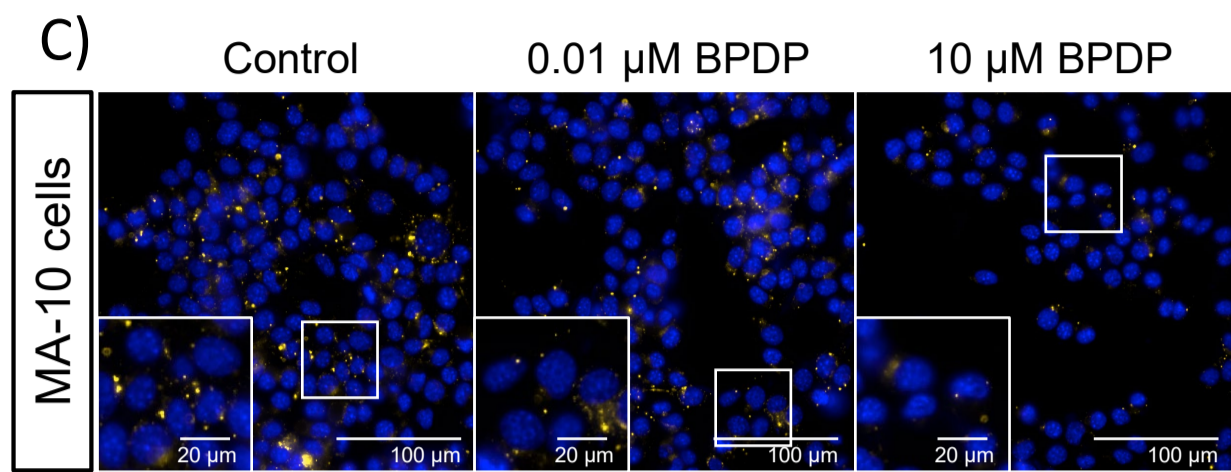
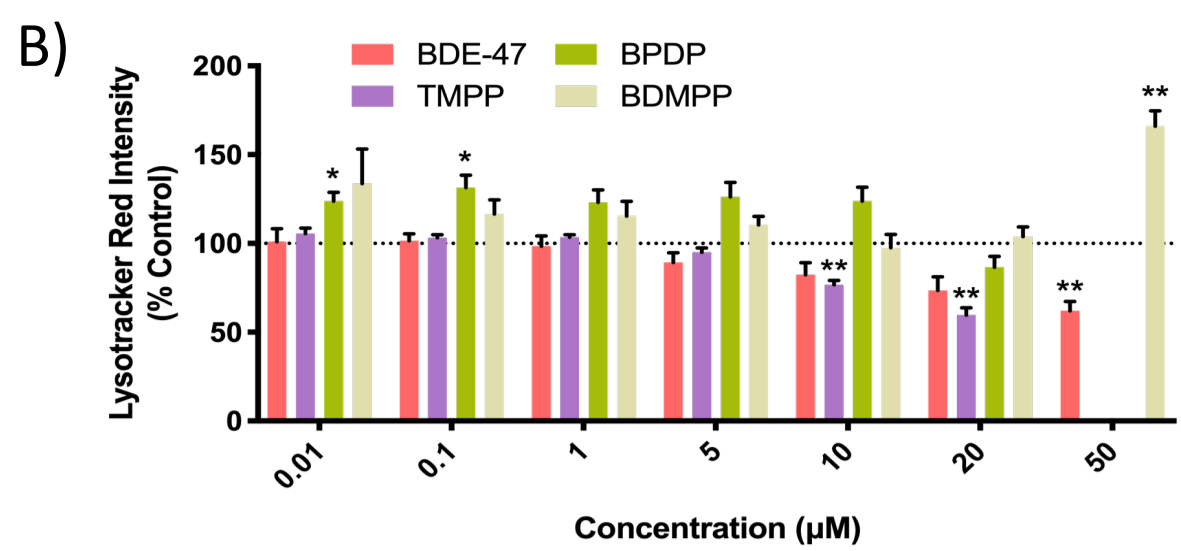
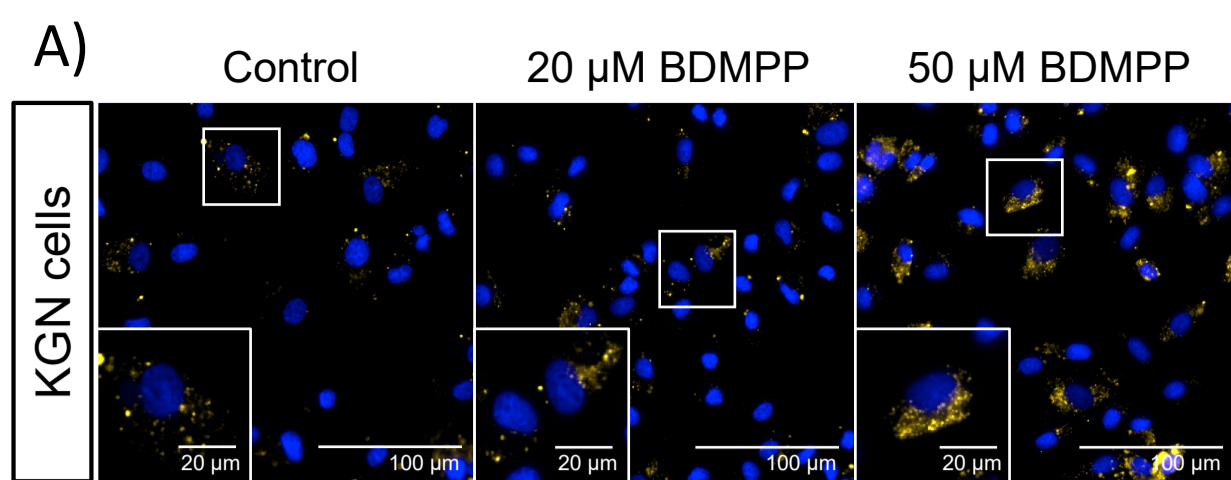


Supplementary figure S1. BDE-47 and OPEs increased the intensity of mitochondrial staining in KGN cells (A and B), MA-10 cells (C and D), and C18-4 cells (E and F). Cells were stained by Hoechst 33342 (blue, stains nuclei), Mitotracker Green (green, stains total mitochondria), and Mitotracker Red (orange, stains active mitochondria) fluorescent dyes for 30 min and visualized by high-content imaging (40X magnification). Scale bars of the insets and the main images denote 20 μm and 100 μm, respectively. Bar graphs show the quantification of the average intensity of Mitotracker Green or Red staining following 48 h exposure to BDE-47 or an OPE. Data are shown as percentages relative to controls; values represent means ± SEM; n = 6-8. One-sample Holm-Bonferroni-corrected t-tests were conducted to determine significant differences from controls (=100): \*p<0.05, \*\*p<0.01; data for concentrations from 0.1 μM to 20 μM, 50 μM or 100 μM of parts of the OPEs are shown. Concentrations that induced more than 30% cell death were excluded from the analyses.



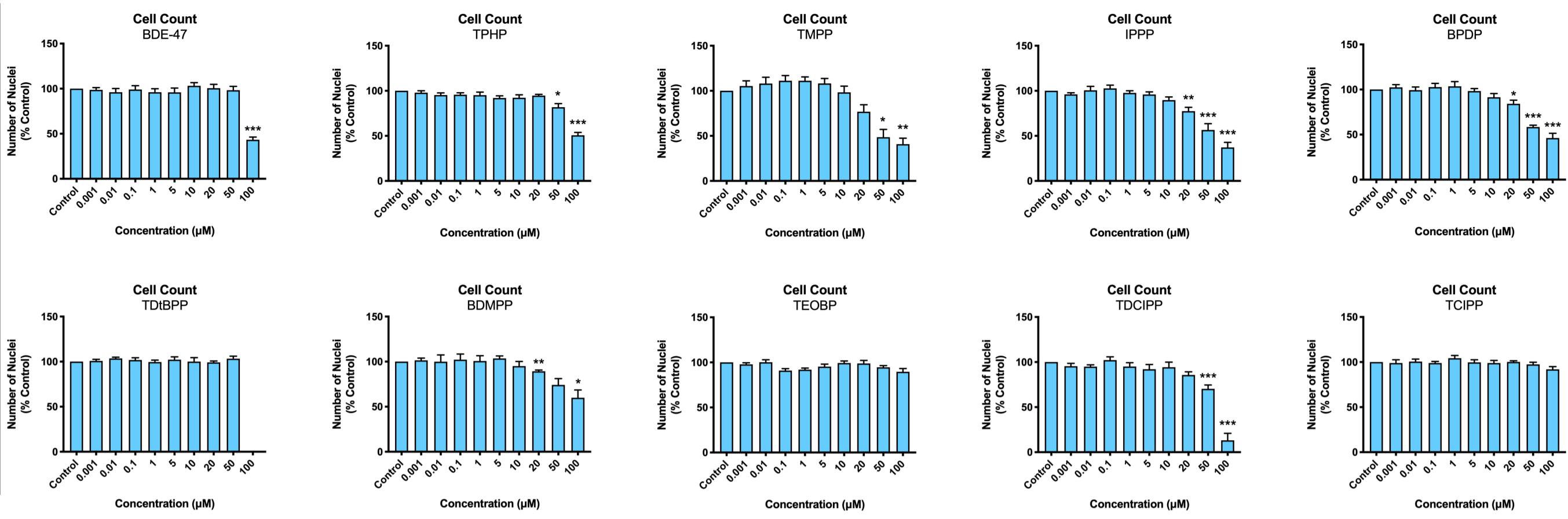
Supplementary figure S2. BDE-47 and OPEs changed the ratio of active to total mitochondria in MA-10 cells (A), and C18-4 cells (B). Cells were stained by Mitotracker Green (stains total mitochondria), and Mitotracker Red (stains active mitochondria) fluorescent dyes for 30 min and visualized by high-content imaging (40X magnification). The ratio between the intensity of Mitotracker Red and Mitotracker Green, which indicates active/total mitochondria, was calculated. Data are shown as percentages relative to controls; values represent means  $\pm$  SEM;  $n = 8$ . One-sample Holm-Bonferroni-corrected t-tests were conducted to determine significant differences from controls ( $=100$ ): \* $p < 0.05$ , \*\* $p < 0.01$ ; data for concentrations from 0.1  $\mu\text{M}$  to 20  $\mu\text{M}$  are shown. Concentrations that induced more than 30% cell death were excluded from the analyses.



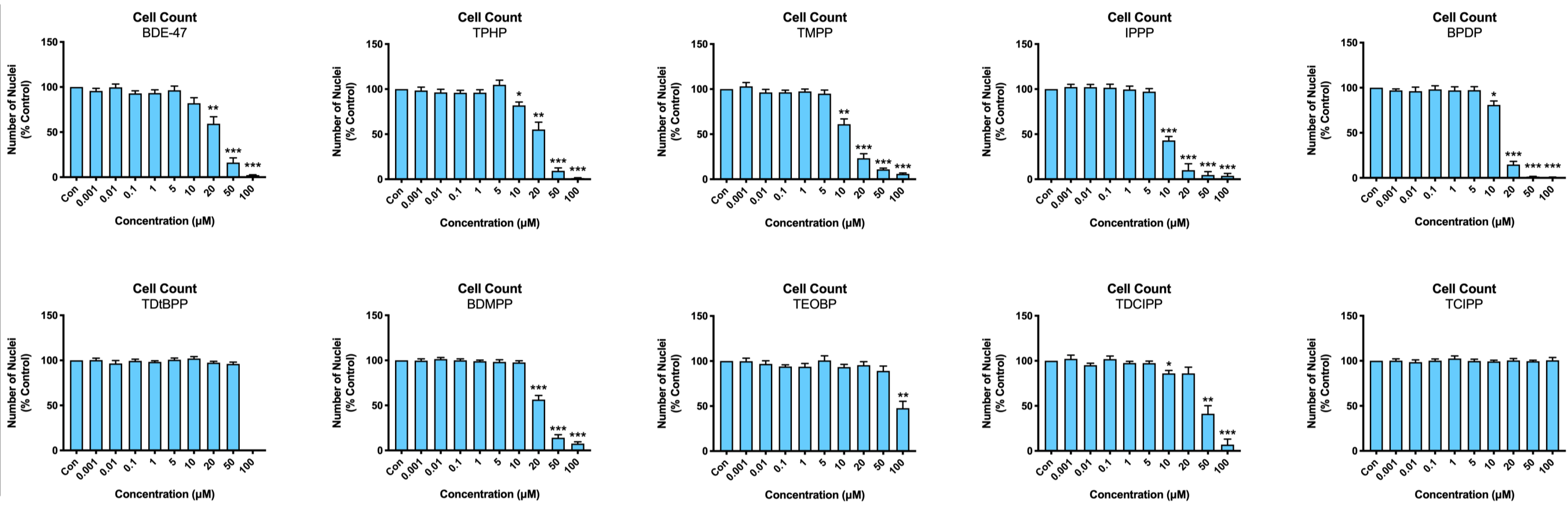


Supplementary figure S3. BDE-47 and OPEs affected the intensity of Lysotracker Red staining in KGN cells (A and B), MA-10 cells (C and D), and C18-4 cells (E and F). Cells were stained by Hoechst 33342 (blue, stains nuclei) and Lysotracker Red (yellow, stains lysosomes) fluorescent dyes for 30 min and visualized by high-content imaging (40X magnification). Scale bars of the insets and the main images denote 20  $\mu\text{m}$  and 100  $\mu\text{m}$ , respectively. Bar graphs show the quantification of the average Lysotracker Red staining intensity following exposure for 48 h to BDE-47 or an OPE. Data are shown as percentages relative to controls; values represent means  $\pm$  SEM; n = 6-8. One-sample Holm-Bonferroni-corrected t-tests were conducted to determine significant differences from control (=100): \*p<0.05, \*\*p<0.01, \*\*\*p<0.001; data for concentrations from 0.1  $\mu\text{M}$  to 50 $\mu\text{M}$  or 100  $\mu\text{M}$  are shown. Concentrations that induced more than 30% cell death were excluded from the analyses.

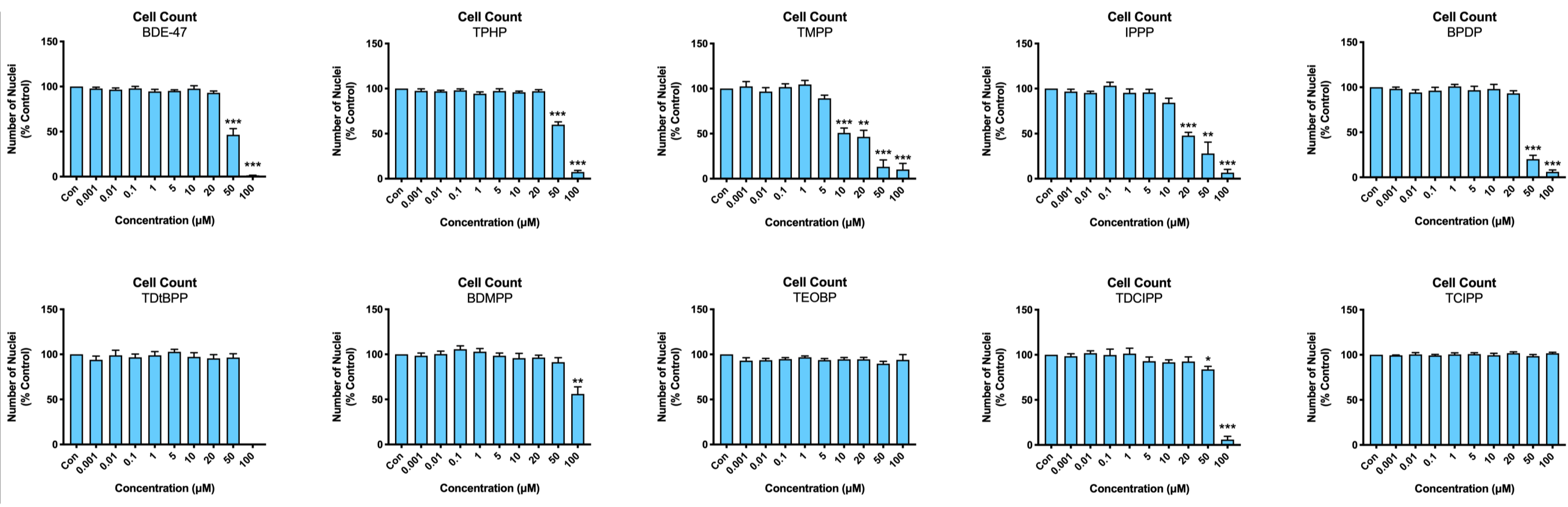
KGN cells



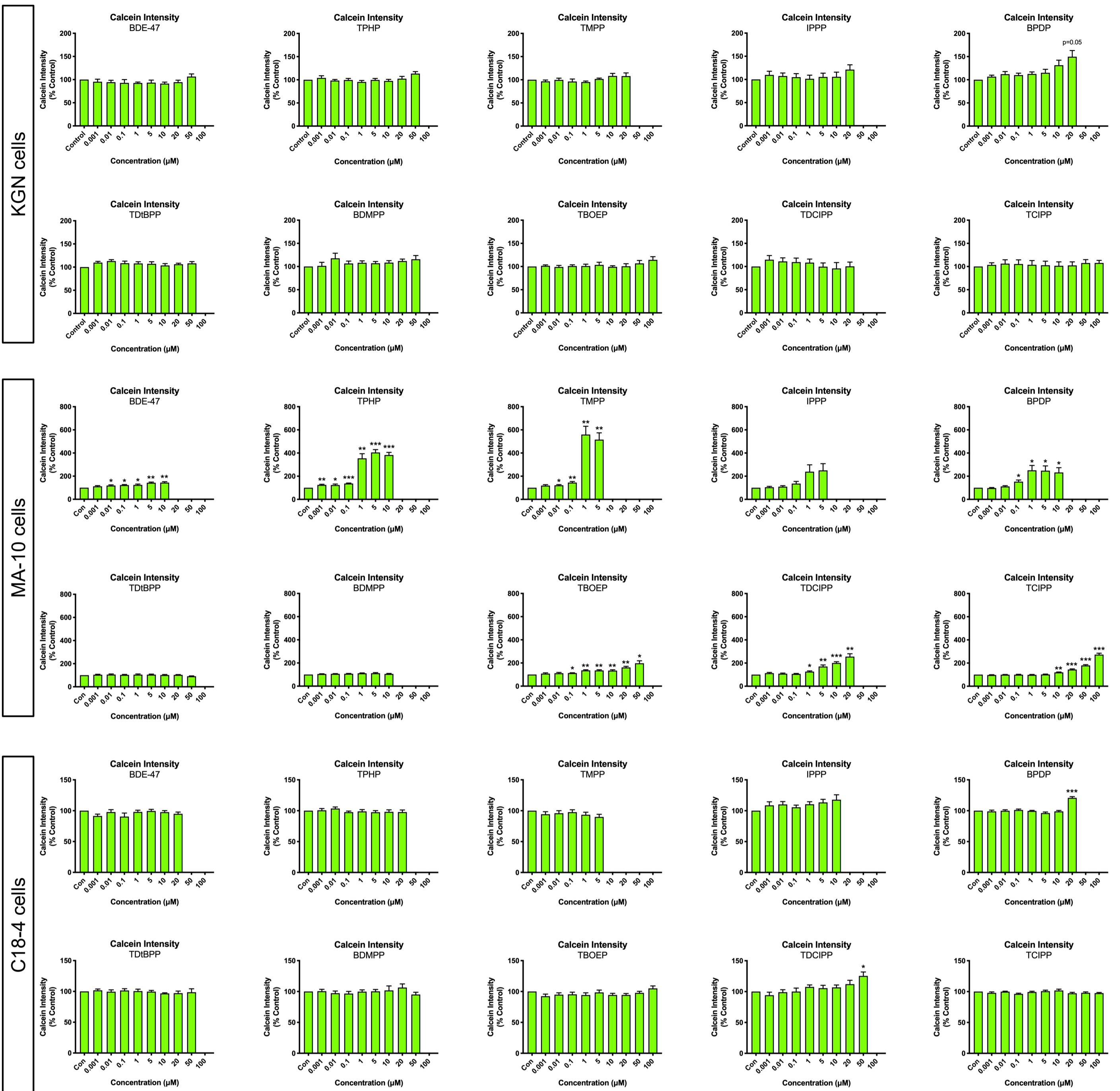
MA-10 cells



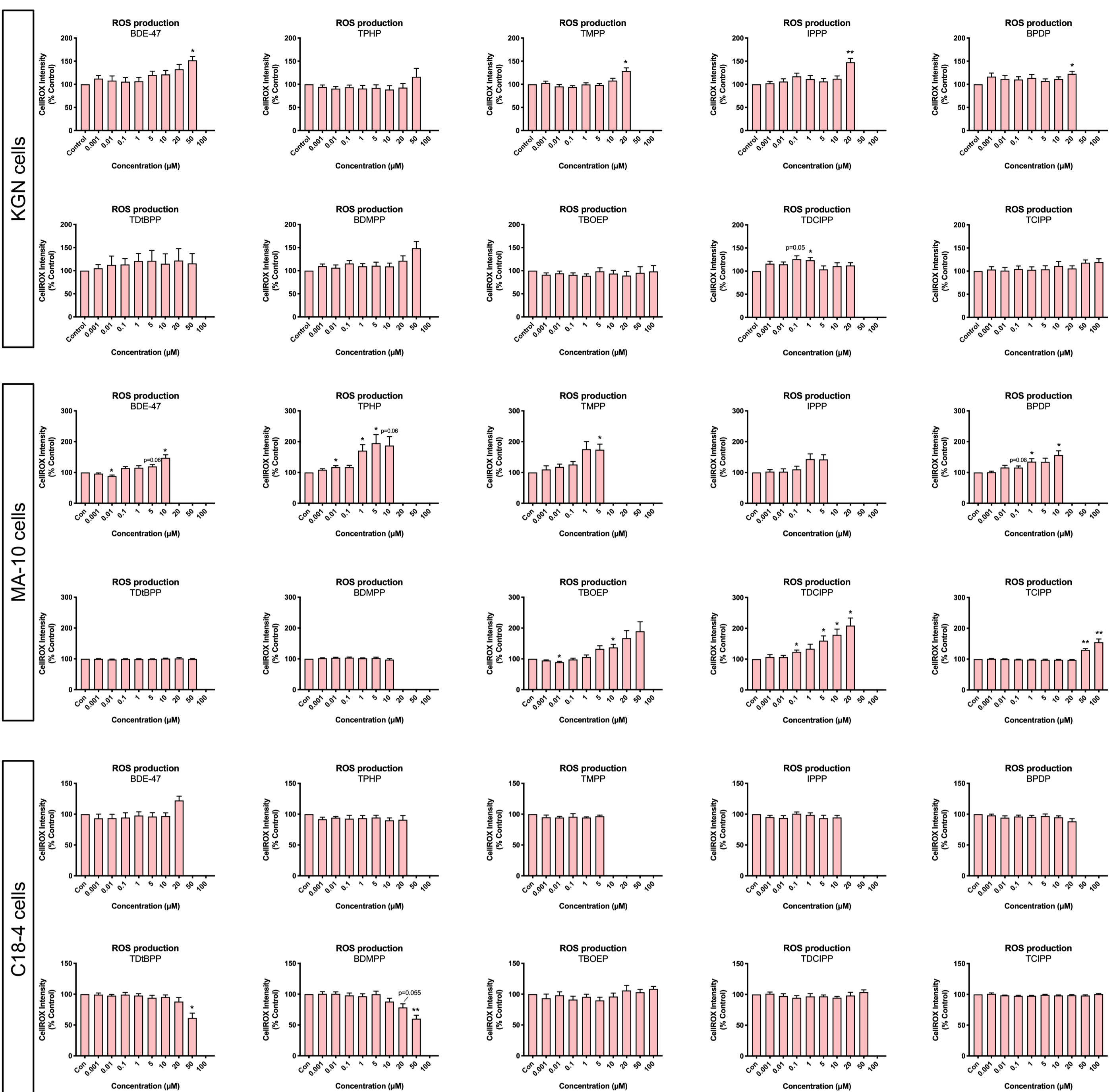
C18-4 cells



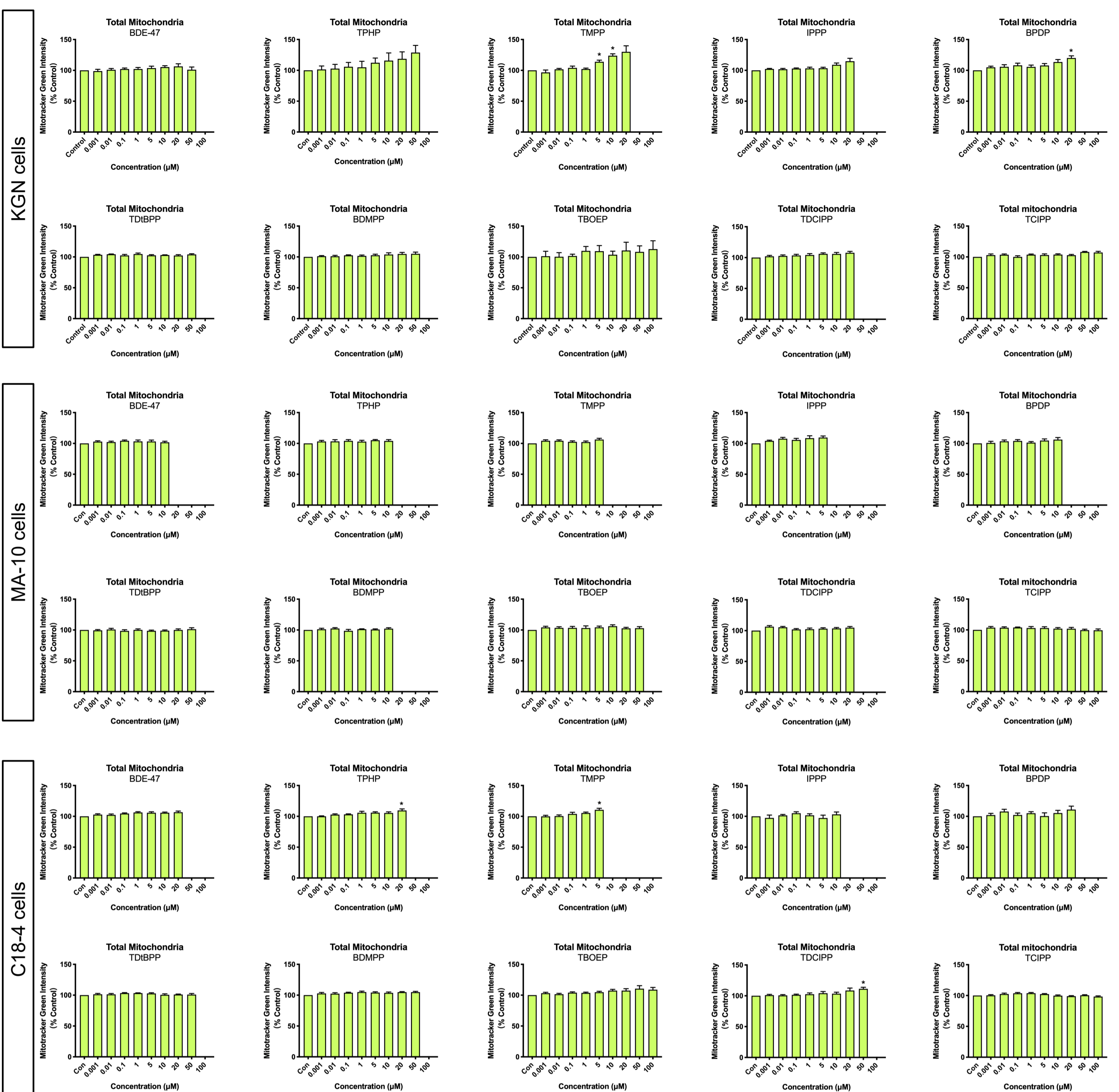
Supplementary figure S4. Cytotoxicity of BDE-47 and OPEs in KGN human granulosa cells, MA-10 mouse Leydig cells, and C18-4 mouse spermatogonial cells. Cells were exposed to one of the chemicals for 48 h; numbers of Hoechst 33342 stained nuclei were quantified using Operetta high-content imaging system (40X magnification). Bar graphs show the effects of BDE-47 and OPEs tested on cell counts. Data are shown as percentages relative to controls; values represent means  $\pm$  SEM; n = 6-8. One-sample Holm-Bonferroni-corrected t-tests were conducted to determine significant differences from controls (=100): \* $p < 0.05$ , \*\* $p < 0.01$ , \*\*\* $p < 0.001$ . Concentrations that induced more than 30% cell death were excluded from the analyses.



Supplementary figure S5. The effects of BDE-47 and OPEs on Calcein-AM staining intensity in KGN human granulosa cells, MA-10 mouse Leydig cells, and C18-4 mouse spermatogonial cells. Cells were stained by Hoechst 33342 (stains nuclei) and Calcein-AM (an indicator of cell viability) fluorescent dyes for 30 min and visualized by high-content imaging (40X magnification). Bar graphs show the quantification of Calcein-AM staining intensity following exposure for 48 h to BDE-47 or an OPE. Data are shown as percentages relative to controls; values represent means  $\pm$  SEM; n = 6-8. One-sample Holm-Bonferroni-corrected t-tests were conducted to determine significant differences from controls (=100): \*p<0.05, \*\*p<0.01, \*\*\*p<0.001. Concentrations that induced more than 30% cell death were excluded from the analyses.

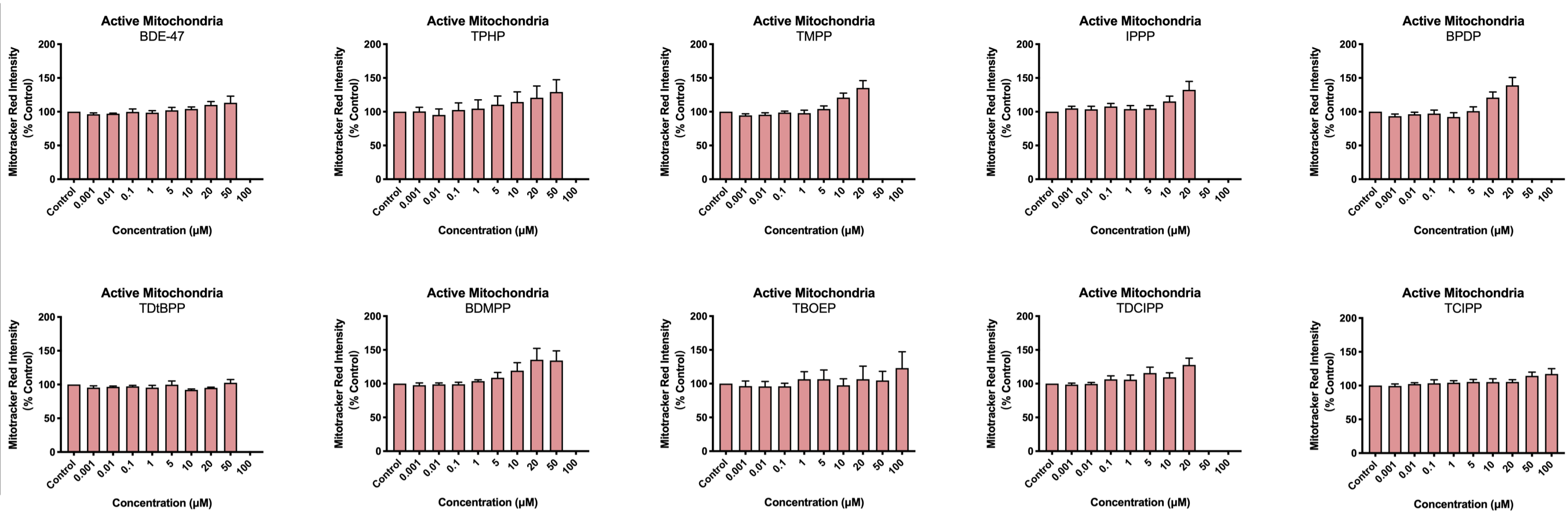


Supplementary figure S6. The effects of BDE-47 and OPEs on the production of reactive oxygen species (ROS) in KGN human granulosa cells, MA-10 mouse Leydig cells, and C18-4 mouse spermatogonial cells. Cells were stained by Hoechst 33342 (blue, stains nuclei) and CellROX (an indicator of oxidative stress) fluorescent dyes for 30 min and visualized by high-content imaging (40X magnification). Bar graphs show the quantification of CellROX staining intensity following exposure for 48 h to BDE-47 or an OPE. Data are shown as percentages relative to controls; values represent means  $\pm$  SEM; n = 6-8. One-sample Holm-Bonferroni-corrected t-tests were conducted to determine significant differences from controls (=100): \*p<0.05, \*\*p<0.01, \*\*\*p<0.001. Concentrations that induced more than 30% cell death were excluded from the analyses.

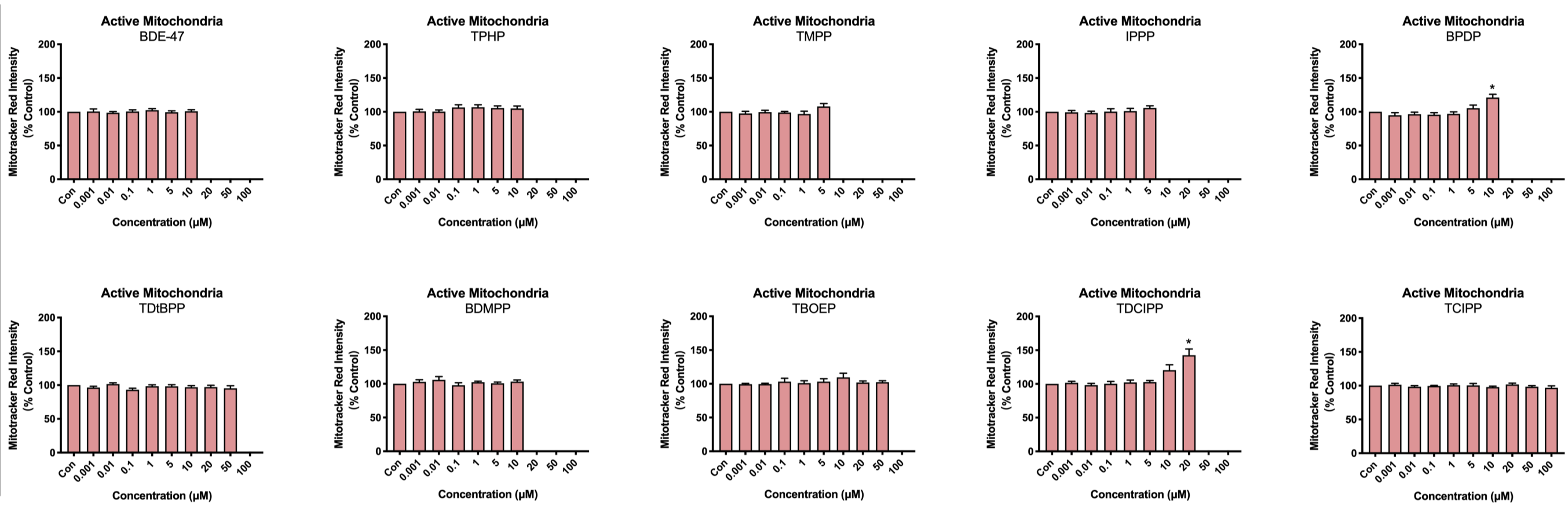


Supplementary figure S7. The effects of BDE-47 and OPEs on total mitochondrial mass in KGN human granulosa cells, MA-10 mouse Leydig cells, and C18-4 mouse spermatogonial cells. Cells were stained by Hoechst 33342 (stains nuclei), Mitotracker Green (stains total mitochondria) fluorescent dyes for 30 min and visualized by high-content imaging (40X magnification). Bar graphs show the quantification of Mitotracker Green staining intensity following exposure for 48 h to BDE-47 or an OPE. Data are shown as percentages relative to controls; values represent means  $\pm$  SEM; n = 6-8. One-sample Holm-Bonferroni-corrected t-tests were conducted to determine significant differences from controls (=100): \* $p < 0.05$ , \*\* $p < 0.01$ , \*\*\* $p < 0.001$ . Concentrations that induced more than 30% cell death were excluded from the analyses.

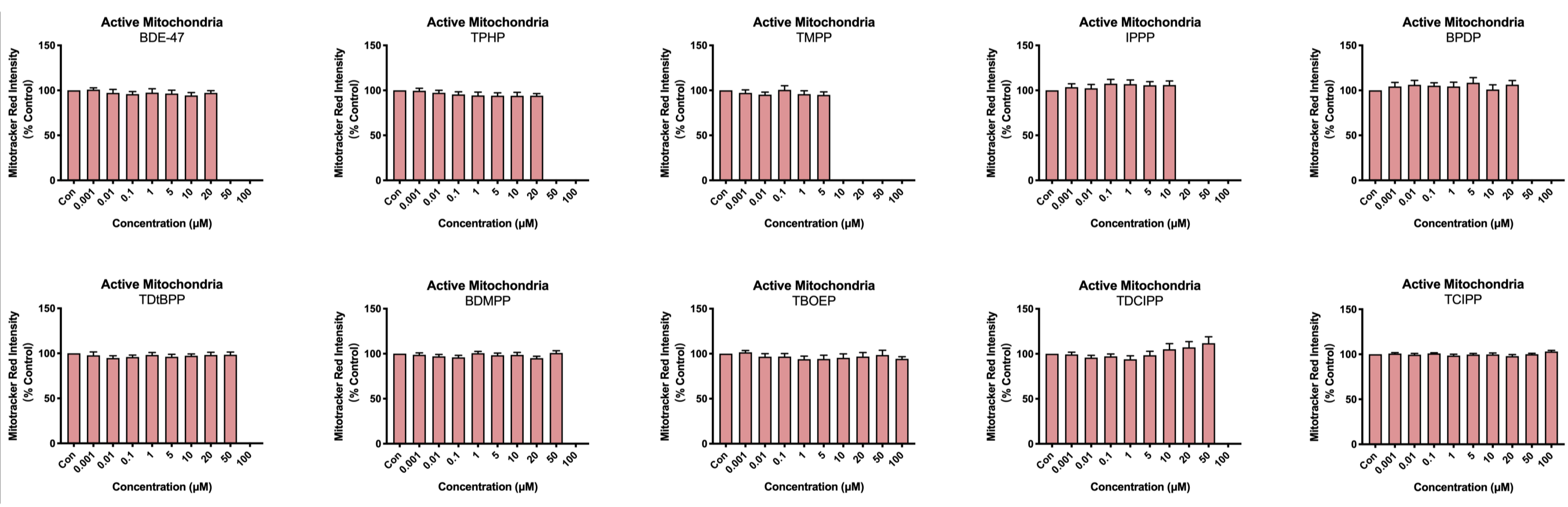
KGN cells



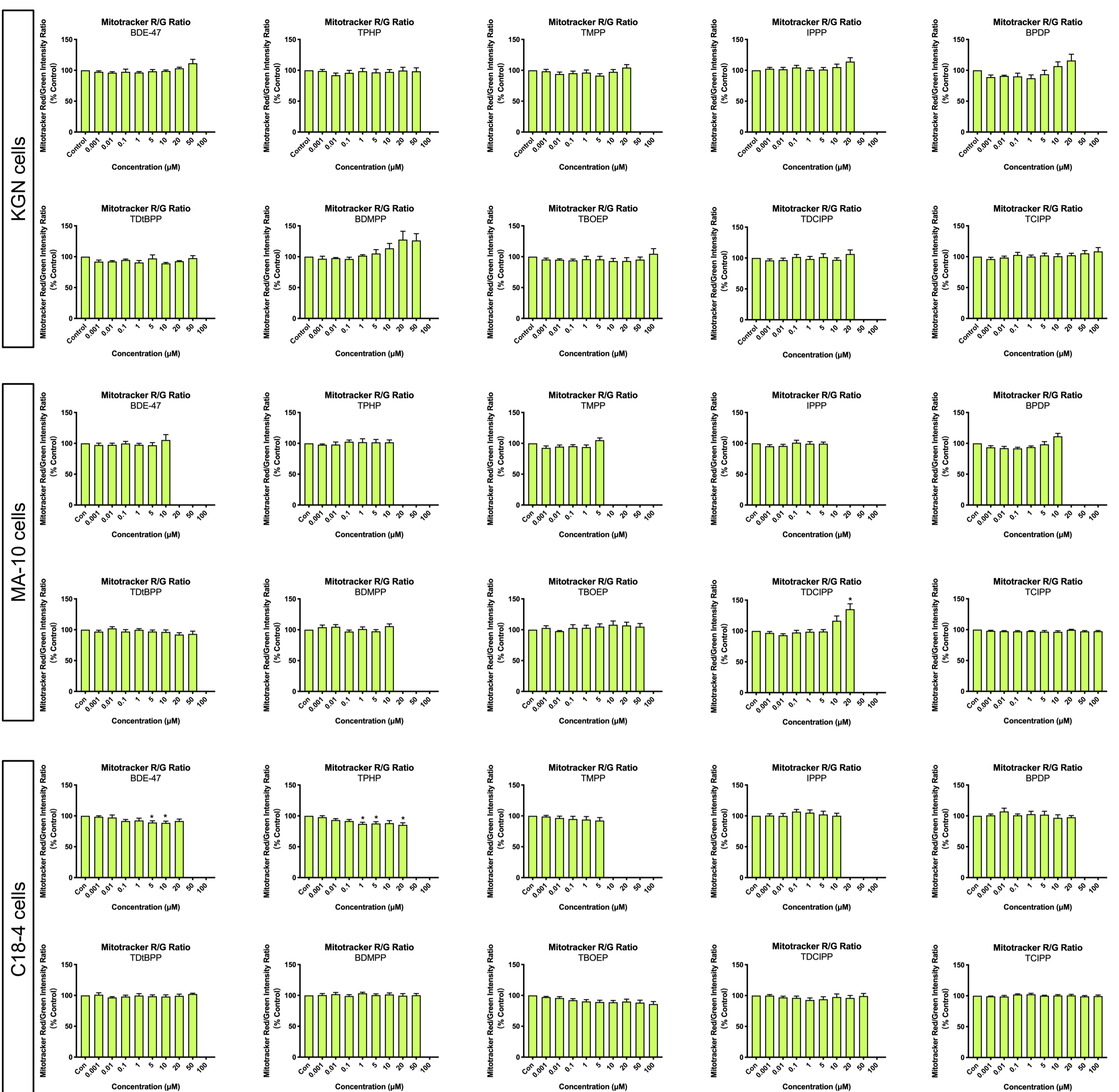
MA-10 cells



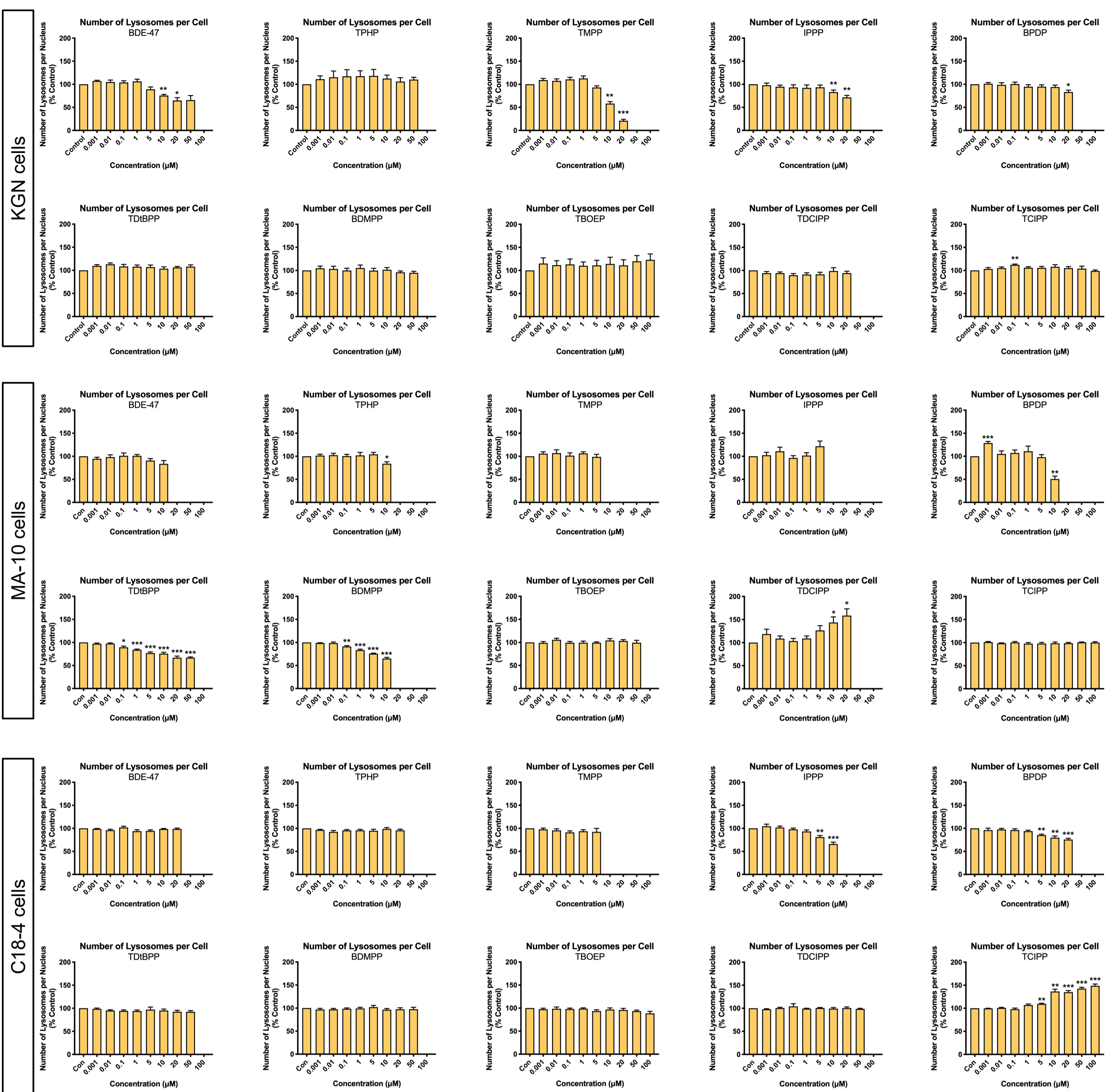
C18-4 cells



Supplementary figure S8. The effects of BDE-47 and OPEs on active mitochondria in KGN human granulosa cells, MA-10 mouse Leydig cells, and C18-4 mouse spermatogonial cells. Cells were stained by Hoechst 33342 (stains nuclei), Mitotracker Red (stains active mitochondria) fluorescent dyes for 30 min and visualized by high-content imaging (40X magnification). Bar graphs show the quantification of Mitotracker Red staining intensity following exposure for 48 h to BDE-47 or an OPE. Data are shown as percentages relative to controls; values represent means  $\pm$  SEM;  $n = 6-8$ . One-sample Holm-Bonferroni-corrected  $t$ -tests were conducted to determine significant differences from controls ( $=100$ ): \* $p < 0.05$ , \*\* $p < 0.01$ , \*\*\* $p < 0.001$ . Concentrations that induced more than 30% cell death were excluded from the analyses.



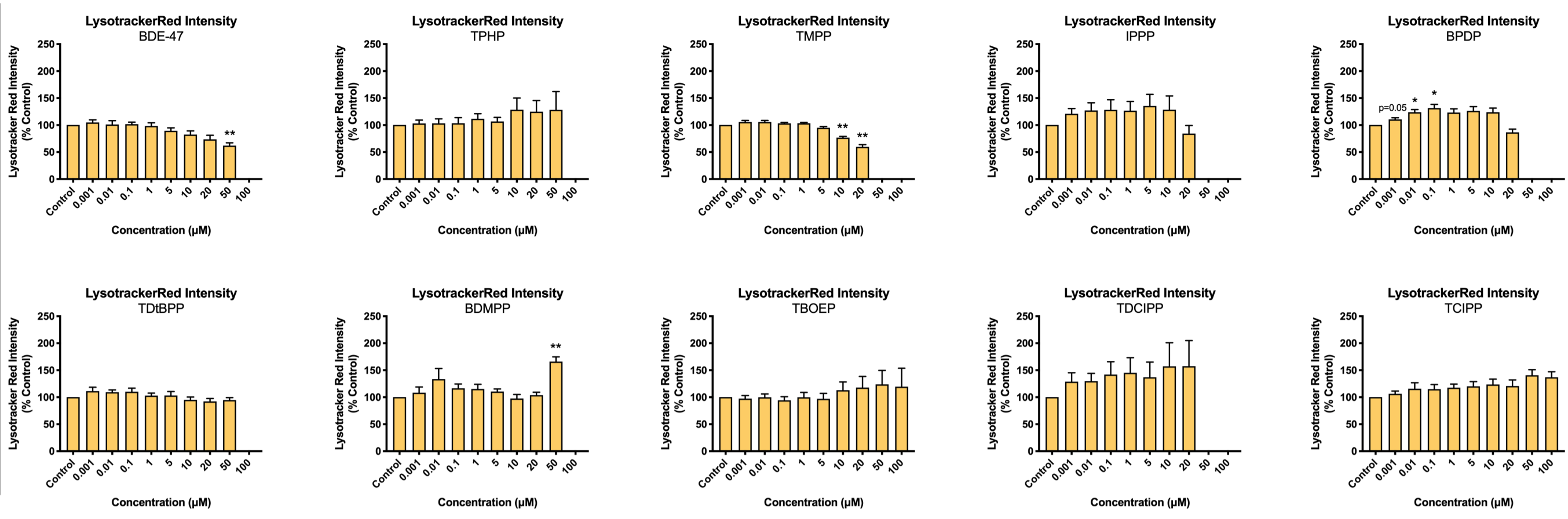
Supplementary figure S9. The effects of BDE-47 and OPEs on the ratio of active to total mitochondria in KGN human granulosa cells, MA-10 mouse Leydig cells, and C18-4 mouse spermatogonial cells. Cells were stained by Hoechst 33342 (stains nuclei), Mitotracker Green (stains total mitochondria), and Mitotracker Red (stains active mitochondria) fluorescent dyes for 30 min and visualized by high-content imaging (40X magnification). Bar graphs show the ratio between the intensity of Mitotracker Red and Mitotracker Green (i.e., R/G ratio). Data are shown as percentages relative to controls; values represent means  $\pm$  SEM;  $n = 6-8$ . One-sample Holm-Bonferroni-corrected t-tests were conducted to determine significant differences from controls (=100): \* $p < 0.05$ , \*\* $p < 0.01$ , \*\*\* $p < 0.001$ . Concentrations that induced more than 30% cell death were excluded from the analyses.



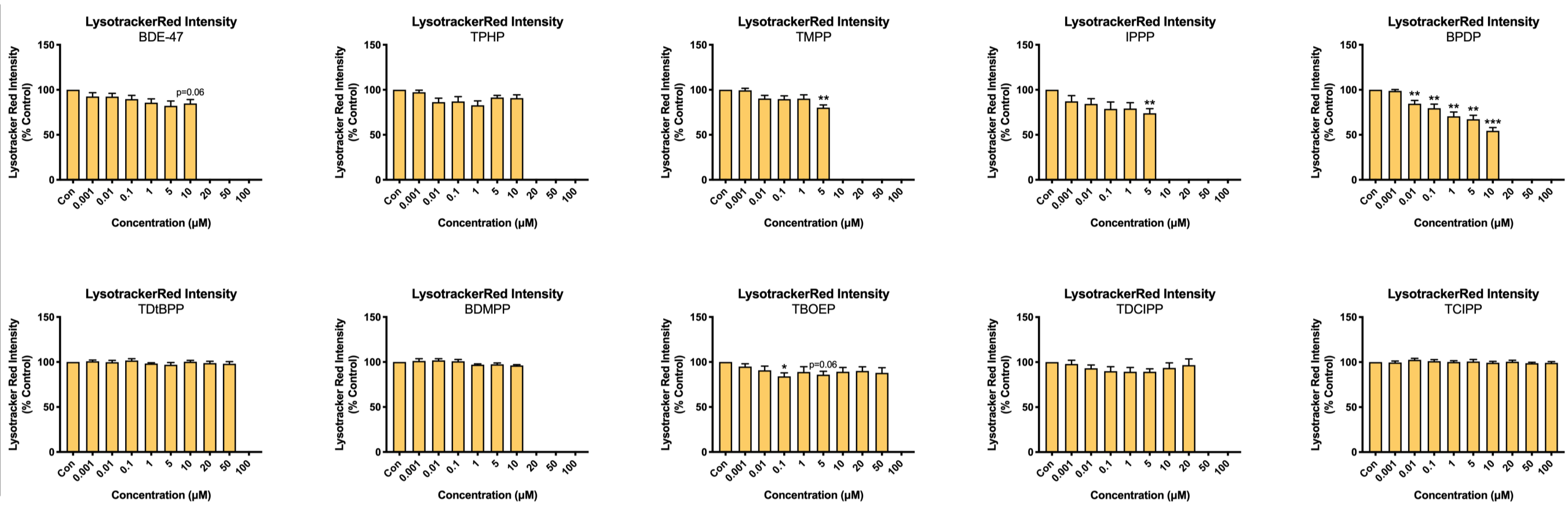
Supplementary figure S10. The effects of BDE-47 and OPEs on the average numbers of lysosomes in KGN human granulosa cells, MA-10 mouse Leydig cells, and C18-4 mouse spermatogonial cells. Cells were stained by Hoechst 33342 (stains nuclei) and LysoTracker Red (stains lysosomes) fluorescent dyes for 30 min and visualized by high-content imaging (40X magnification). Bar graphs show the numbers of lysosomes per nucleus following exposure for 48 h to BDE-47 or an OPE. Data are shown as percentages relative to controls; values represent means  $\pm$  SEM; n = 6-8. One-sample Holm-Bonferroni-corrected t-tests were conducted to determine significant differences from controls (=100): \* $p$ <0.05, \*\* $p$ <0.01, \*\*\* $p$ <0.001. Concentrations that induced more than 30% cell death were excluded from the analyses.



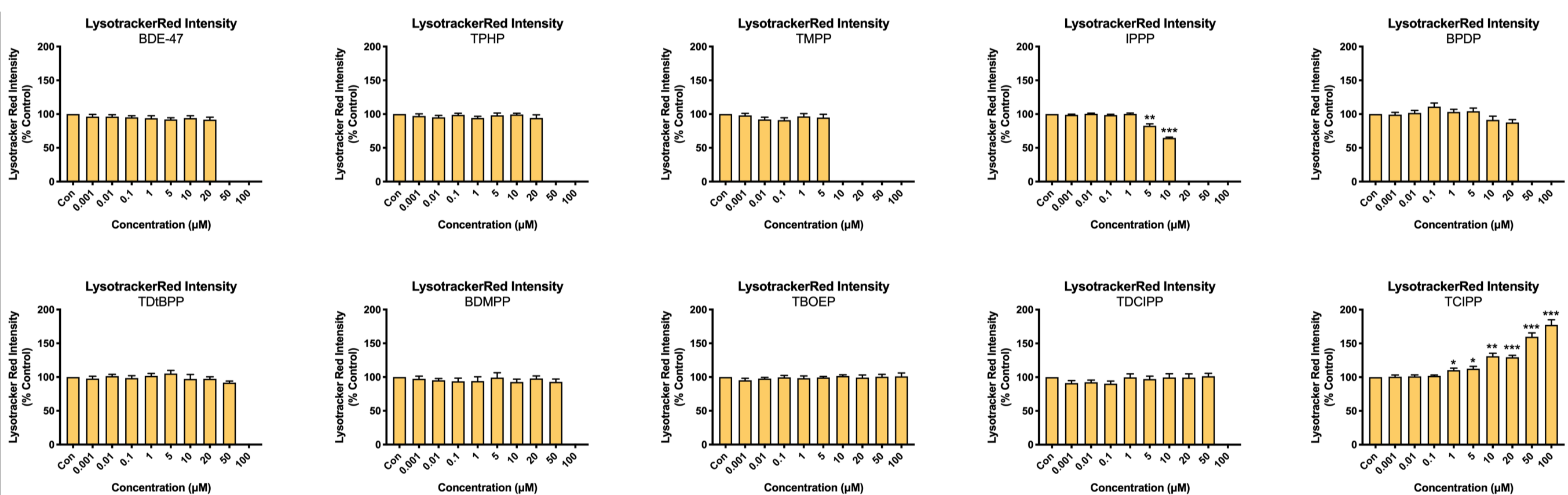
KGn cells



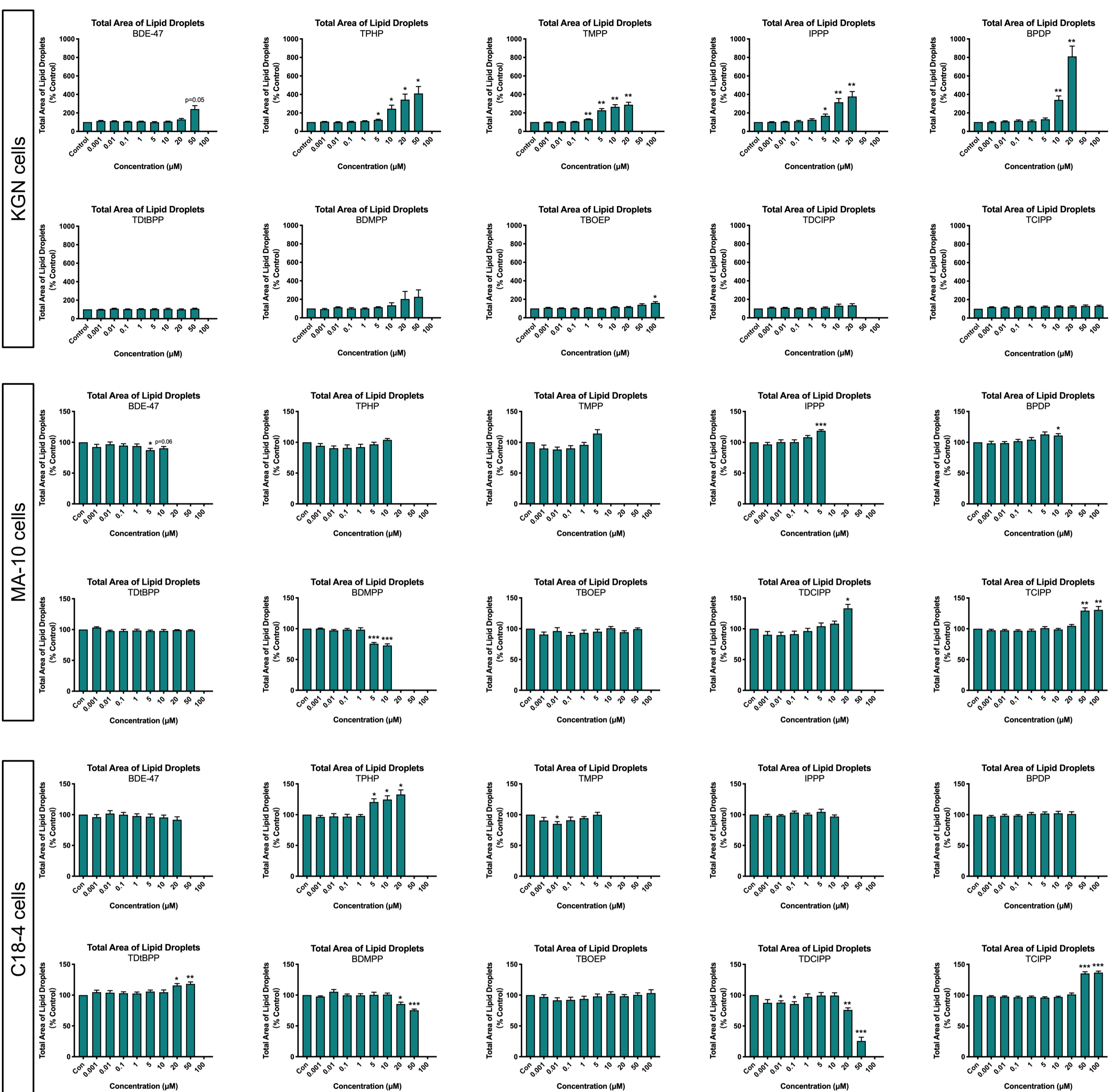
MA-10 cells



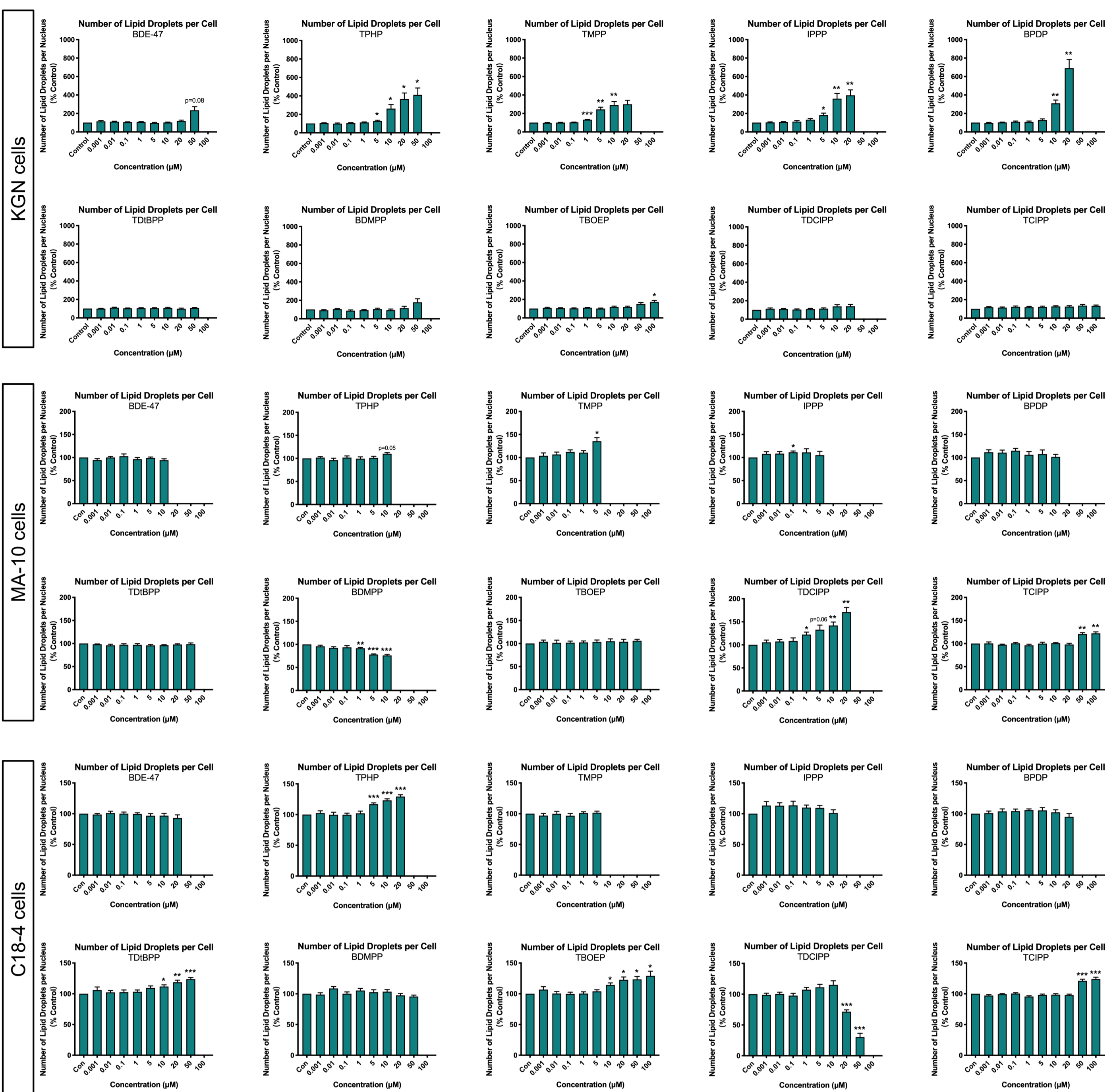
C18-4 cells



Supplementary figure S11. The effects of BDE-47 and OPEs on the intensity of Lysotracker Red staining in KGn human granulosa cells, MA-10 mouse Leydig cells, and C18-4 mouse spermatogonial cells. Cells were stained by Hoechst 33342 (stains nuclei) and Lysotracker Red (stains lysosomes) fluorescent dyes for 30 min and visualized by high-content imaging (40X magnification). Bar graphs show the quantification of Lysotracker Red staining intensity following exposure for 48 h to BDE-47 or an OPE. Data are shown as percentages relative to controls; values represent means ± SEM; n = 6-8. One-sample Holm-Bonferroni-corrected t-tests were conducted to determine significant differences from controls (=100): \*p<0.05, \*\*p<0.01, \*\*\*p<0.001. Concentrations that induced more than 30% cell death were excluded from the analyses.

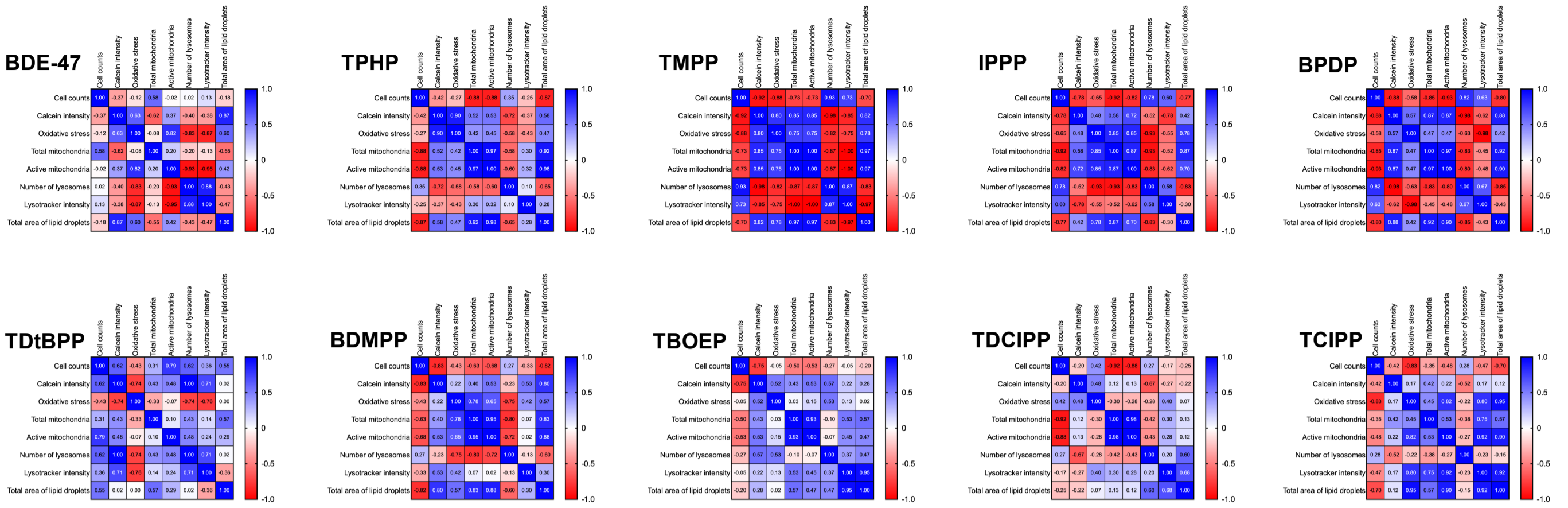


Supplementary figure S13. The effects of BDE-47 and OPEs on the total area of lipid droplets in KGN human granulosa cells, MA-10 mouse Leydig cells, and C18-4 mouse spermatogonial cells. Nuclei and lipid droplets in cells were stained by Hoechst 33342 and Nile Red for 30 min and visualized by high-content imaging (40X magnification). Bar graphs show the quantification of total lipid droplet areas following exposure for 48 h to BDE-47 or an OPE. Data are shown as percentages relative to controls; values represent means  $\pm$  SEM; n = 6-8. One-sample Holm-Bonferroni-corrected t-tests were conducted to determine significant differences from controls (=100): \*p<0.05, \*\*p<0.01, \*\*\*p<0.001. Concentrations that induced more than 30% cell death were excluded from the analyses.

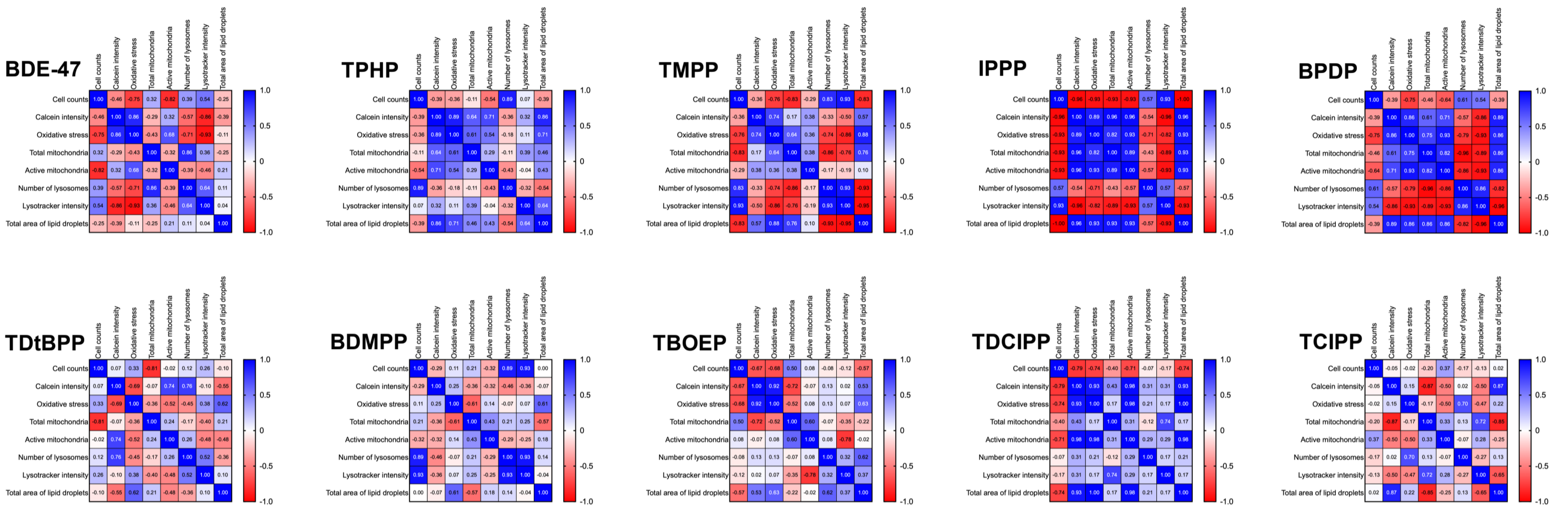


Supplementary figure S14. The effects of BDE-47 and OPEs on the average numbers of lipid droplets in KGN human granulosa cells, MA-10 mouse Leydig cells, and C18-4 mouse spermatogonial cells. Nuclei and lipid droplets in cells were stained by Hoechst 33342 and Nile Red for 30 min and visualized by high-content imaging (40X magnification). Bar graphs show the average numbers of lipid droplets per nucleus following exposure for 48 h to BDE-47 or an OPE. Data are shown as percentages relative to controls; values represent means  $\pm$  SEM; n = 6-8. One-sample Holm-Bonferroni-corrected t-tests were conducted to determine significant differences from controls (=100): \* $p$ <0.05, \*\* $p$ <0.01, \*\*\* $p$ <0.001. Concentrations that induced more than 30% cell death were excluded from the analyses.

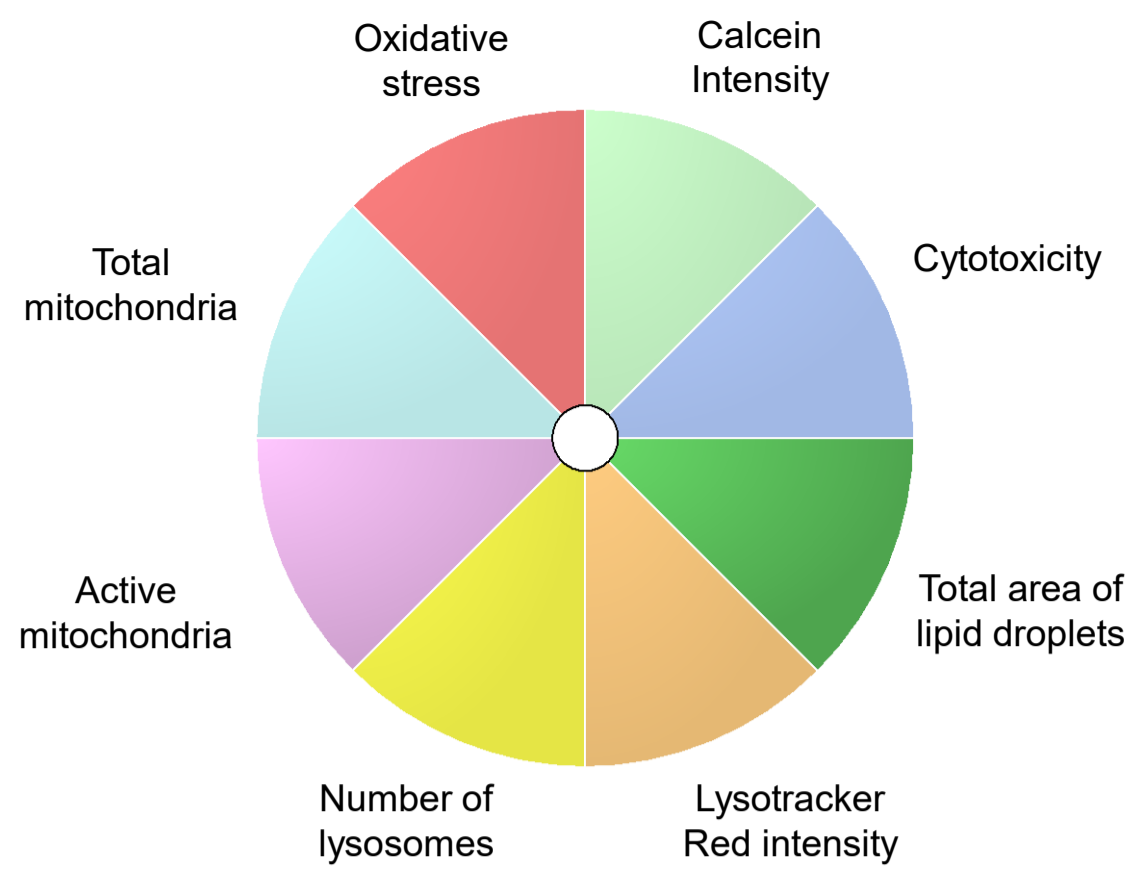
## KGN cells



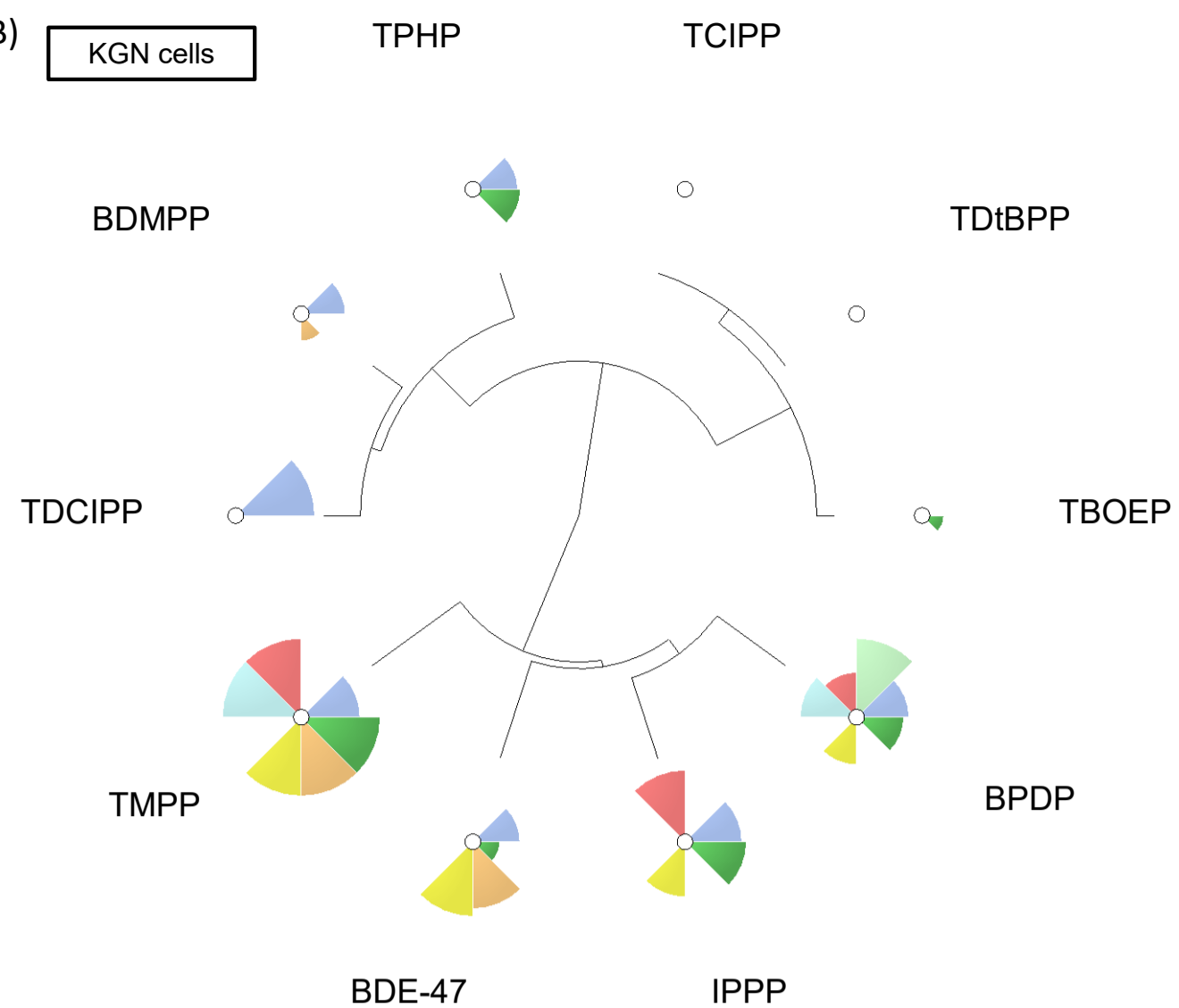
## MA-10 cells



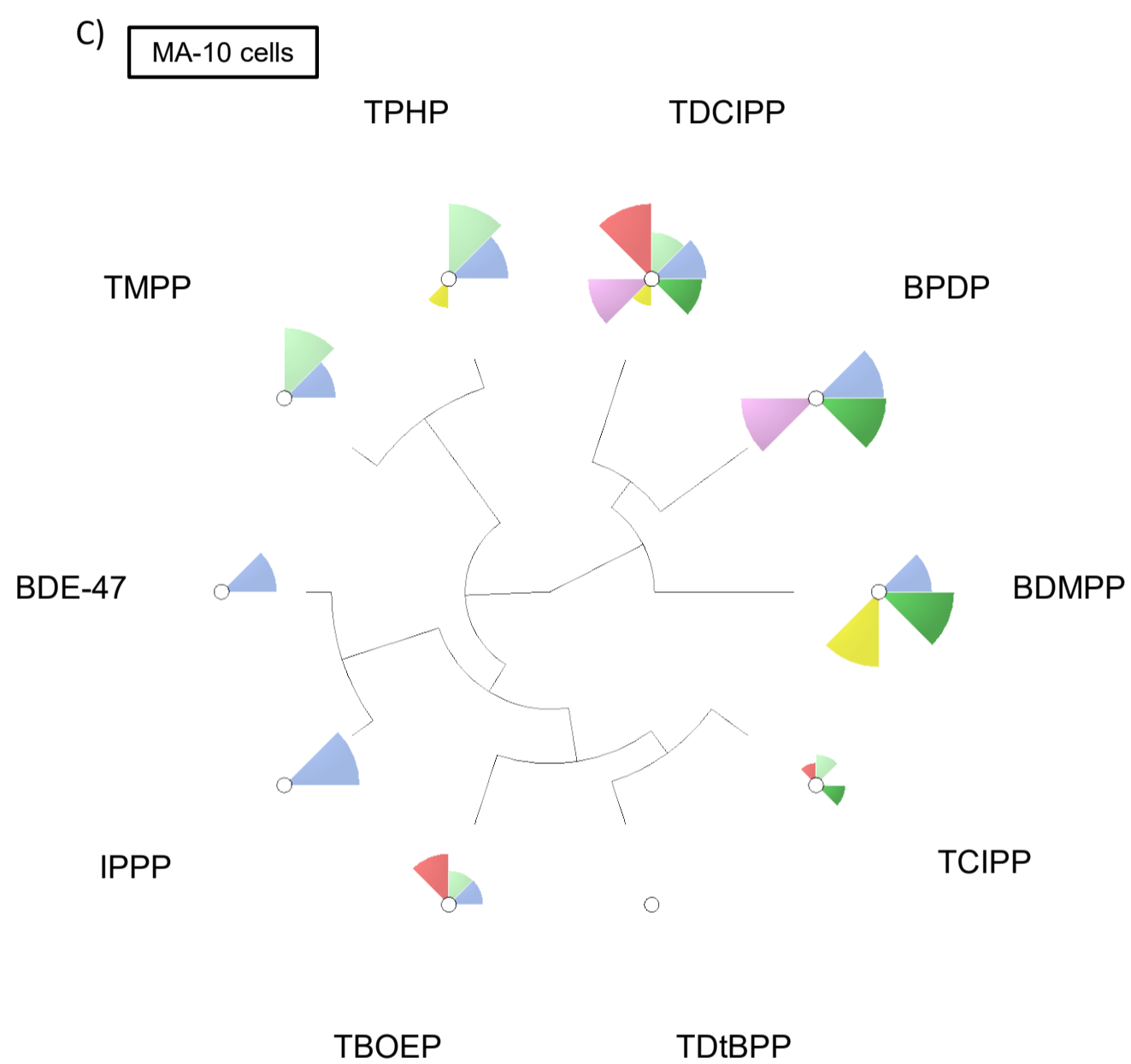
A)



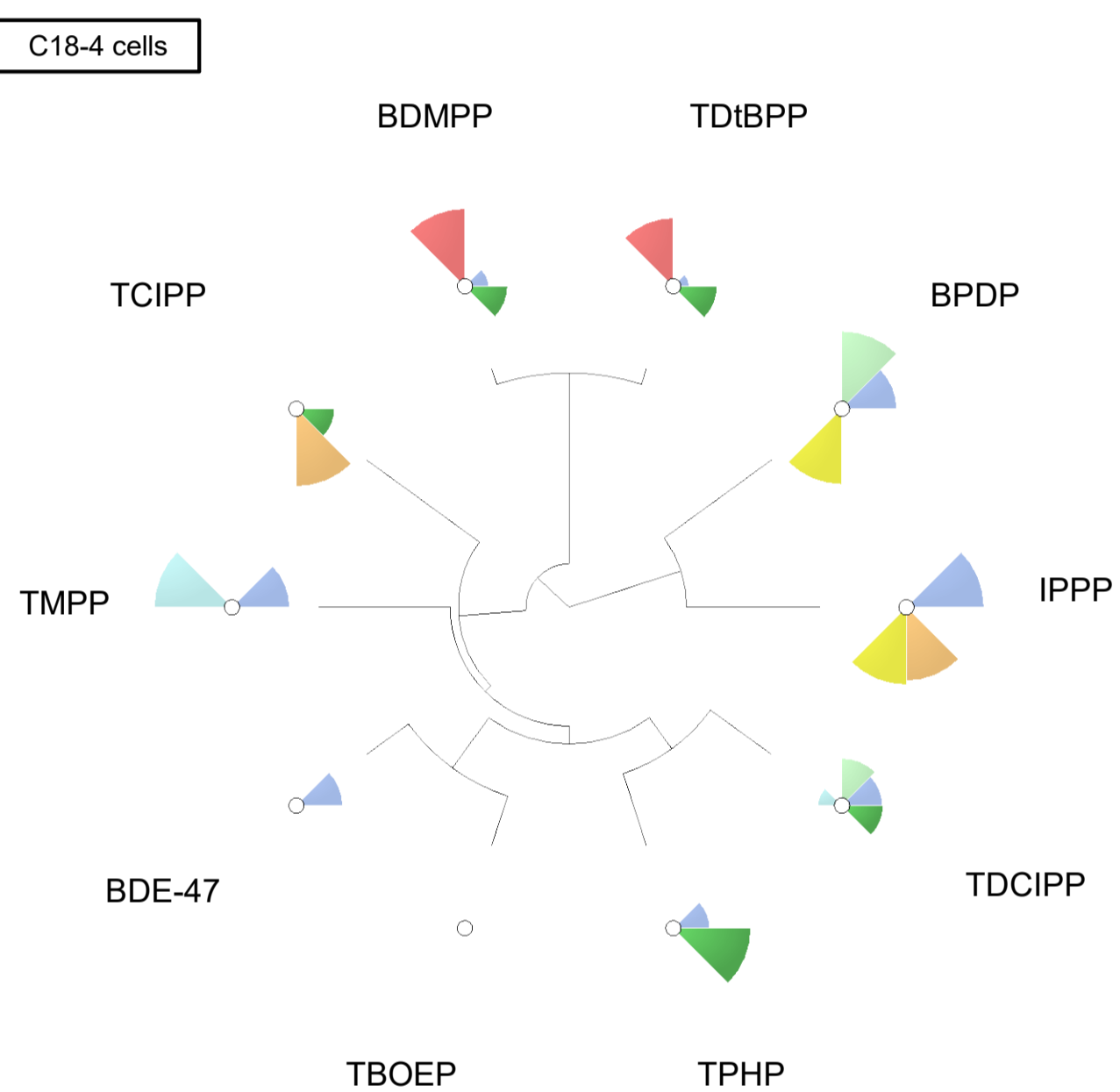
B)



C)



D)



Supplementary figure S16. Clustering analyses (Ward's D method) based on chemical-specific ToxPi profiles in KGN cells (B), MA-10 cells (C), and C18-4 cells (D). Color preview for the ToxPi profiles is shown in (A).